

## Central Lancashire Online Knowledge (CLoK)

Title	An Investigation into the Effects of Outer Membrane Vesicles and Lipopolysaccharide of Porphyromonas gingivalis on Blood-Brain Barrier Integrity, Permeability, and Disruption of Scaffolding Proteins in a Human in vitro Model
Type	Article
URL	<a href="https://clock.uclan.ac.uk/40482/">https://clock.uclan.ac.uk/40482/</a>
DOI	##doi##
Date	2022
Citation	Pritchard, Anna orcid iconORCID: 0000-0002-6280-7008, Fabian, Zsolt orcid iconORCID: 0000-0002-4973-9872, Lawrence, Clare Louise orcid iconORCID: 0000-0003-0170-0079, Morton, Glyn, Crean, Stjohn orcid iconORCID: 0000-0001-9336-8549 and Alder, Jane Elizabeth orcid iconORCID: 0000-0003-4463-0349 (2022) An Investigation into the Effects of Outer Membrane Vesicles and Lipopolysaccharide of Porphyromonas gingivalis on Blood-Brain Barrier Integrity, Permeability, and Disruption of Scaffolding Proteins in a Human in vitro Model. Journal of Alzheimer's Disease . pp. 1-22. ISSN 1387-2877
Creators	Pritchard, Anna, Fabian, Zsolt, Lawrence, Clare Louise, Morton, Glyn, Crean, Stjohn and Alder, Jane Elizabeth

It is advisable to refer to the publisher's version if you intend to cite from the work. ##doi##

For information about Research at UCLan please go to <http://www.uclan.ac.uk/research/>

All outputs in CLoK are protected by Intellectual Property Rights law, including Copyright law. Copyright, IPR and Moral Rights for the works on this site are retained by the individual authors and/or other copyright owners. Terms and conditions for use of this material are defined in the <http://clock.uclan.ac.uk/policies/>

1                   **An investigation into the effects of outer membrane vesicles and**  
2                   **Lipopolysaccharide (LPS) of *Porphyromonas gingivalis* on blood**  
3                   **brain barrier integrity, permeability and disruption of scaffolding**  
4                   **proteins in a human in vitro model.**

5  
6                   Anna Barlach **Pritchard**<sup>a</sup>, Zsolt **Fabian**<sup>b</sup>, Clare L **Lawrence**<sup>c</sup>, Glyn **Morton**<sup>d</sup>,  
7                   StJohn **Crean**<sup>a</sup> and Jane E **Alder**<sup>c</sup>

8                   <sup>a</sup> Brain and Behaviour Centre, Faculty of Clinical and Biomedical Sciences,  
9                   School of Dentistry, University of Central Lancashire, Preston, UK.

10                  <sup>b</sup> School of Medicine, University of Central Lancashire, Preston, UK

11                  <sup>c</sup> Brain and Behaviour Centre, Faculty of Clinical and Biomedical Sciences,  
12                  School of Pharmacy and Biomedical Sciences, University of Central  
13                  Lancashire, Preston, UK.

14                  <sup>d</sup> School of Forensic and Investigative Science, University of Central  
15                  Lancashire, Preston, UK

16                  \*Correspondence to Anna Barlach Pritchard, Brain and Behaviour Centre,  
17                  Faculty of Clinical and Biomedical Sciences, School of Dentistry, University of  
18                  Central Lancashire, Preston, UK. Tel.: +44 0 1772 895906; E-mail:  
19                  abpritchard@uclan.ac.uk

21  
22  
23  
24  
25  
26  
27  
28  
29  
30  
31  
32  
33  
34  
35  
36  
37  
38  
39  
40  
41  
42  
43  
44  
45  
46

ABSTRACT

The journey and effects of gum disease key pathogens such as *Porphyromonas gingivalis* (*P.gingivalis*) and its virulence factors to and on the central nervous system is of great interest with respect to development of therapeutics and preventative strategies. The role of chronic infections and associated inflammation is important as both are known to weaken the first line of defence for the brain; the blood brain barrier (BBB). The focus of this study is to utilise an established human *in vitro* BBB model to evaluate the effects of *P.gingivalis* virulence factors Lipopolysaccharide (LPS) and outer membrane vesicles (OMVs) on a primary-derived human model representing the neuro vascular unit of the BBB. Changes to the integrity of the BBB after application of *P.gingivalis* LPS and OMVs were investigated and correlated with transport of LPS . Additionally, the effect of *P.gingivalis* LPS and OMVs on human brain microvascular endothelial cells in monolayer was evaluated using immunofluorescence microscopy. The integrity of the BBB model was weakened by application of *P.gingivalis* LPS and OMVs, as measured by a decrease in electrical resistance (TEER) and a recovery deficit was seen in comparison to the controls. Application of *P.gingivalis* OMVs to a monoculture of human brain microvascular endothelial cells (HBMEC) showed disruption of the tight junction zona occludens protein (ZO-1) compared to controls. These findings show that the integrity of healthy cells and potentially their tight junctions of the human BBB could be weakened by association with *P.gingivalis* virulence factors LPS and OMVs containing proteolytic enzymes (gingipains).

Keywords

Blood brain barrier, HBMEC, Alzheimer’s Disease, micro biome, Periodontal disease, *in vitro* BBB model.

47

48 BACKGROUND

49 The concept of a microbial cause or risk factor for neurodegenerating disease such  
50 as sporadic Alzheimer's Disease has gathered momentum in the past decade. Why  
51 some individuals develop sporadic Alzheimer's Disease (AD) while others are  
52 resistant remains unresolved. There is currently no effective treatment for AD or a  
53 way of slowing or stopping the rate of neurodegeneration. What has emerged is a  
54 body of evidence over the past decade which supports a possible microbial role in  
55 the development of neurodegeneration, which includes epidemiological data, post-  
56 mortem and experimental studies. The evidence suggests that microbes potentially  
57 linked to AD may be viral, bacterial or fungal in origin [1,2,3,4]. It is known that there  
58 are multiple risk factors for developing sporadic AD, the most significant being  
59 advanced age [4]. However, the possibility of a microbial role as a causative factor  
60 for AD, opens new possibilities for the discovery of novel preventative measures and  
61 therapeutic targets. Pivotal to the discovery of such novel drug targets is the need to  
62 create research models that are representative of human physiology and disease  
63 state.

64 AD is a chronic neurodegenerative condition which is known to develop over  
65 decades, displaying histological hallmarks of extracellular amyloid- $\beta$  (A $\beta$ ) plaques  
66 and hyper phosphorylated intracellular Tau tangles within the brain parenchyma [5].  
67 AD can also be considered as a chronic inflammatory disease and has been linked to  
68 inflammatory events [6] such as traumatic brain injury or vascular disease, with  
69 subsequent activation of the immune system and release of appropriate  
70 inflammatory mediators purposely to protect the brain. If an individual predisposed  
71 either through age, genetics, illness or lifestyle habits (smoking, diet, exercise) [7],

72 develops a persistent inflammatory trigger, then this can establish a chronic tissue  
73 reaction with devastating toxic effects at a cellular level [8] and even initiating a path  
74 to recognised AD pathology [6]. Sporadic AD presents late in life in individuals who  
75 may not have an overt history of an acute inflammatory event, but the pathological  
76 end point is the same [8]. The search for a trigger of raised levels of pro-  
77 inflammatory mediators and oxidative stress, identified in AD patients goes on.

78 The detection of multiple microbials in post-mortem brains from AD individuals and  
79 the notion that A $\beta$  can behave as an anti-microbial peptide [9,10] raises the  
80 possibility that an external [chronic] assault on brain tissues, for example infection  
81 by the oral periodontal disease bacteria *Porphyromonas gingivalis* (*P.gingivalis*),  
82 could cumulatively damage brain tissue and even lead to low level  
83 neurodegenerative changes decades before a clinical diagnosis of AD presents [8].

84 Periodontal disease (PD) is a chronic infection caused by bacteria in the gums around  
85 teeth represented by microbial dysbiosis and tissue destruction [11,12]. PD has been  
86 linked to other organ specific disease such as Alzheimer's Disease, atherosclerosis,  
87 and diabetes mellitus [13,14]. The progression of PD in humans is determined by  
88 microbiological, environmental and genetic factors (multiple polymorphisms) [15]. It  
89 can go undiagnosed for years and even if oral hygiene measures are improved, there  
90 is a potential of daily bacteraemia (s) of periodontal pathogens when chewing foods  
91 or cleaning teeth [16]. It is this chronic bacterial load in the circulation which is  
92 proposed to contribute to a systemic chronic inflammatory state.

93 *P.gingivalis*, an anaerobic Gram-negative coccobacillus, is a key pathogen of PD and  
94 has numerous mechanisms which can affect the surroundings tissues including i)  
95 endotoxin or lipopolysaccharide (LPS) mainly located on the outer membrane and ii)  
96 via release of outer membrane vesicles (OMVs) by the Type IX secretion system. The

97 working hypothesis the authors propose is that a chronic assault on the BBB from  
98 circulating periodontal pathogens and/or their associated virulence factors could  
99 lead to disruption of the integrity of the barrier (either by increased permeability or  
100 reduction in clearance). Whilst there is some evidence to support the concept it  
101 remains incompletely evidenced in humans and *P.gingivalis* cells have not yet been  
102 found in the brain of AD patients or test animals[13]. However, human post-mortem  
103 studies have found evidence of *P.gingivalis* DNA and virulence factors, LPS and  
104 proteases secreted by *P.gingivalis* (gingipains), in the brains of AD individuals  
105 [17,18]. *In vivo* animal studies, investigating the administration of *P.gingivalis*  
106 associated virulence factors have shown that these substances travel to and settle in  
107 the animal's brain [19,20]. Illievski et al., (2018) [20] showed that infection of mice  
108 with *P.gingivalis* induced neuroinflammation and appeared to induce the deposition  
109 of intracerebral A $\beta$  protein, drawing similarities to the human AD pathology. It  
110 remains unclear however, whether the reason for the A $\beta$  protein seen in the brain of  
111 the test animals was due to a direct cerebral invasion of intact *P.gingivalis*, its  
112 virulence factors such as gingipains or an indirect effect from the inflammatory  
113 mediators of systemic infection [20]. The authors suggest two pathways for  
114 *P.gingivalis* inducing neurodegenerative changes. Either i) *P.gingivalis* can access the  
115 brain directly or ii) the bacteria can orchestrate the neurological changes from a  
116 distant site of infection, i.e., the periodontal pockets in the oral cavity. The key  
117 question remains if or how *P.gingivalis* and its virulence factors access brain tissue,  
118 how do they cross the BBB?

#### 119 P.GINGIVALIS AND ASSOCIATED VIRULENCE FACTORS

120 The virulence or invasive ability of a *P.gingivalis* strain can be classified according to  
121 the expression of fimbriae, capsule, LPS and gingipains release [21]. These virulence

122 factors originate from the mother cell but are disseminated wider by release of  
123 OMVs. As an example, the non-capsulated laboratory strain FDC 381 has been  
124 shown to invade carcinoma cells  $10^3$  times more than other *P.gingivalis* strains [21],  
125 though FDC 381 is classed as a less virulent type causing only mild localised  
126 abscesses [22]. These findings highlight two key aspects of *P.gingivalis* behaviour  
127 which have significance for pathological development, the ability of the bacterium to  
128 i) invade tissues and ii) modulate the subsequent immune response of the host.  
129 Furthermore, a variance between different invasive abilities of OMVs from  
130 *P.gingivalis* strains has been attributed to the expression of long fimbriae (not FimA)  
131 and the gingipain adhesive domains in the outer membrane [23]. OMVs of  
132 *P.gingivalis* are highly enriched in the proteolytic gingipains (RgpA/B and Kgp) and  
133 the nano sized spheres also incorporate high concentrations of LPS and fimbriae [24]  
134 which are sustainable in human tissues such as the brain [25]. *P.gingivalis* OMVs,  
135 containing a high concentration of enzymes, are considered to have both harmful  
136 and beneficial roles, enabling *P.gingivalis* to regulate its microenvironment [26].  
137 Internalised OMVs are associated with cell degradation [27] and induction of an  
138 innate immune response with a greater intensity than initiated by the bacteria itself.  
139 Gingipains are also believed to help *P.gingivalis* evade the reach of the immune  
140 system, making *P.gingivalis* so successful in establishing a chronic diseased state  
141 [28].

142 *P.gingivalis* has also been shown to dysregulate dendritic cells by disturbing their  
143 ability toward autophagy and apoptosis [29] endowing this pathogen with an  
144 exceptional ability for self-preservation. Labelled *P.gingivalis* OMVs have also been  
145 shown to be taken up by cortical microglial cells in mice, 24 -48 hours after  
146 peripheral injection highlighting the potential reach of this virulence factor. It has  
147 even been suggested that OMVs may act as a decoy to the host immune system,

148 diverting attention and thus protecting the mother cell from elimination [30],  
149 forming another element of *P.gingivalis*' immune evasive strategy. The size and  
150 proteolytic capacity of the OMVs makes the spread into tissues easier than for the  
151 intact bacteria and OMVs are more likely to survive transport to remote organs.  
152 LPS from the outer membrane of Gram-negative bacteria is a powerful pro-  
153 inflammatory pathogen associated molecular pattern (PAMP) and previous studies  
154 support the capabilities of oral bacterial LPS as an inducer of peripheral  
155 inflammatory responses and as an initiating factor in intracerebral inflammatory  
156 activity [17,20]. The LPS of *P.gingivalis* has been extensively studied in relation to its  
157 pathogenicity, is found in both a soluble and membrane bound form and binds to  
158 TLR4 enhanced by sCD14 [31] activating pro-inflammatory pathways.

#### 159 HUMAN BLOOD BRAIN BARRIER

160 The cells of the blood brain barrier, also described as the neuro vascular unit (NVU),  
161 comprise of endothelial cells, pericytes, astrocytes and neurons [32]. The 400 miles  
162 of capillaries in the human brain [33] makes this the largest potential entry point for  
163 pathogens to the CNS, but its intimate integrity affords a significant barrier. This  
164 integrity arises from; endothelial cell i) intercellular tight junctions displaying high  
165 electrical resistance, limiting any transcytosis compared to peripheral endothelial  
166 cells [34], ii) lack of fenestrae (transcellular pores) and iii) shared basement  
167 membrane with pericytes with reduced pinocytic activity. Human *in vitro* BBB  
168 models are used to investigate both disease and drug interactions of this interface  
169 providing a very valuable tool to assess permeability, transport and transendothelial  
170 electrical resistance (TEER), as well as expression of proteins [35]. The benefits of  
171 using a human primary-derived cell-based model are numerous and combinations of



172 cells of the NVU have been validated and standardised, for a comprehensive review  
173 see [35].

174 The integrity of the BBB is reduced naturally as we age [36] and multiple neurological  
175 conditions have been associated with a “leaky” BBB [34], including AD and  
176 Parkinson’s disease, implying the importance its role in brain homeostasis and risk of  
177 age-related neurodegeneration [13]. Many of these neurological conditions also  
178 present with a raised level of systemic pro-inflammatory cytokines which are also  
179 thought capable of contributing to weakening in the barrier’s integument [37,38].

180 Studies in mouse apolipoprotein E (ApoE) knock-out models [39] and humans who  
181 express the E4 isoform of (APOE4), the most prevalent predisposed genetic risk  
182 factor for AD, also show accelerated breakdown of the BBB structure and  
183 degeneration of brain capillary pericytes required for barrier integrity [40].

184

185

#### 186 CNS PERMEATION BY *P.GINGIVALIS* AND ASSOCIATED VIRULENCE FACTORS

187 The journey for *P.gingivalis* and associated virulence factors, from the periodontal  
188 pocket to the central nervous system (CNS) has been suggested to follow a number  
189 of possible routes, such as tracking along the trigeminal or olfactory nerves [41], by  
190 being internalised by peripheral immune cells and subsequently transferring to the  
191 CNS or finally arriving in the systemic circulation at the BBB or the blood  
192 cerebrospinal fluid barrier (BCSFB) [42].

193 Both Gram negative and positive bacteria can cross at the BBB and BCSFB interfaces  
194 to the CNS by transcytosis. Bacteria such as *Neisseria.meningitidis* are able to open  
195 endothelial intercellular junctions to cross the CNS barriers in acute infection [42]

196 and *P.gingivalis* gingipains have been shown to degrade the epithelial JAM-1 protein  
197 [43] and induce cell adhesion molecule cleavage and apoptosis in human  
198 microvascular endothelial cells [44]. *P.gingivalis* has also been demonstrated to  
199 induce apoptosis and tight junction disruption in cultured human lung epithelial cells  
200 [45]. It is not clear however, whether these findings were caused by the bacteria or  
201 its virulence factors.

202

### 203 NEUROINFLAMMATION

204 If *P.gingivalis* was shown to induce damage to the BBB of an individual, some time  
205 before any neuroinflammation becomes clinically detectable, then the authors  
206 propose that bacteria or associated virulence factors must be capable of damaging  
207 the BBB enough to trigger a change either to its integrity allowing an influx of  
208 inflammagens and/or weakening the barrier's normal clearance strategies. If the  
209 initial causal factor for the pro-inflammatory state is not resolved, then any  
210 subsequent effects of chronic oxidative stress on the NVU cells can lead to loss of  
211 redox balance, alterations in numbers and differentiation of T-cells subpopulations  
212 and subsequent loss of regulation of the neuroinflammatory response [46]. Animal  
213 studies for example have demonstrated that LPS can incite oxidative stress,  
214 activation of glial cells and tight junction degradation in the NVU and surrounding  
215 cells [47,48].

216 Though much research has been undertaken to understand the events at the BBB in  
217 diseased individuals [47,48,49] and the effects of *P.gingivalis* and its virulence  
218 factors on tissues, very little is known about what effect this bacterium and its  
219 virulence factors exert on the cells of the blood-brain interface especially in the pre-  
220 clinical stages.

221 The authors thus pose the question, could a persistent level of *P.gingivalis* virulence  
222 factors in the circulation, renewed daily by chewing or tooth brushing [16] be  
223 sufficient to cause damage to the BBB in an otherwise healthy state?

224 The aim of this study was to investigate how the *P.gingivalis* virulence factors LPS  
225 and OMVs affected primary human cells in an *in vitro* BBB in the absence of the  
226 bacterial mother cell. This was assessed by investigating i) BBB integrity by  
227 transendothelial electrical resistance across the barrier, ii) how barrier permeability  
228 to fluorescent labelled LPS and dextrans was altered by the presence of *P.gingivalis*  
229 LPS and OMVs and iii) how LPS and OMVs interacted with the human brain  
230 microvascular endothelial cells.

231

## 232 METHODS

### 233 BBB MODEL

234 Primary-derived cell lines of human brain microvascular endothelial cells (HBMECs)  
235 (Neuromics USA) at passage 3, human brain vascular pericytes (HBVP) (ScienCell,  
236 USA) at passage 3 and human astrocytes (HA) cells (ScienCell, USA) at passage 3  
237 were grown in flasks pre-coated with either AlphaBioCoat solution (Neuromics, USA)  
238 or Poly-L-Lysine 10 mg/ml (Sciencell, USA). Cells were cultured in complete  
239 endothelial cell growth basal medium (EBM) (Lonza, Switzerland), complete pericyte  
240 medium (PM) (Sciencell, USA) and astrocyte basal medium (ABM) (Lonza,  
241 Switzerland) with addition of human serum (Life Science Group, UK). The cells were  
242 grown to a confluency of 85-90% in humidified incubator at 37 °C, 5 % CO<sub>2</sub>. The  
243 media was changed in all culture vessels every 48 hours until 50% confluent after  
244 this point every 24 hours. Trypsin (TrypLeexpress, Gibco, Thermofisher, USA) and

245 Hank's Balanced Salt Solution (Gibco, ThermoFisher, USA) were used for passaging  
246 cells. All observations of the cells were carried out under an inverted light  
247 microscope (Leica DMIL light microscope from Leica Microsystems GmbH, Germany).  
248 The viability and counting of the cells were assessed by using 1:1 Trypan Blue 0.4%  
249 (Sigma-Aldrich) and a haemocytometer [50,51]. Transwell™ multiple well plate with  
250 permeable polycarbonate membrane inserts (6.5 mm, 8.0 µm pore) (Corning, Fisher,  
251 UK) were coated with fibronectin (Sigma, UK) The HA and HBVP were seeded on the  
252 basolateral side of the insert and the HBMEC on the apical side [50]. The cells were  
253 maintained with medium of equal volume of PM, ABM and EBM (Lonza, Switzerland  
254 and Sciencell, USA) in a 37 °C humidified incubator under 5 % CO<sub>2</sub>.

#### 255 BBB INTEGRITY

256 After 4 days the integrity of the barrier model was tested by measuring the trans-  
257 endothelial electrical resistance (TEER) with an EVOM-2 instrument (WPI, UK). As the  
258 barrier becomes established the TEER value rise expressed in Ohm/cm<sup>2</sup> [52]. The  
259 triculture *in-vitro* BBB model was considered ready for testing when the TEER values  
260 reached an average of 260 Ohm/cm<sup>2</sup> [50,53]. The triculture barrier integrity were  
261 also assessed by application of FITC dextran 3-5 kD, which was added to the apical  
262 compartment of the inserts and incubated for specific time periods according to the  
263 test protocols in the 37 °C humidified incubator under 5 % CO<sub>2</sub>. At the specified time  
264 points in the test protocol samples were removed from the basolateral  
265 compartment and measured in a GENios Pro plate reader (Tecan, Austria) at 490 nm  
266 excitation and 520 nm emission (gain 40, 22°C). Standard curves were produced  
267 from standard solutions of FITC 3-5 kDa and FITC-conjugated LPS in the range 0.04 to  
268 100 µg/ml.

#### 269 CULTURE OF BACTERIA

270 *P.gingivalis* ATCC-BAA-1703 (strain FDC 381) was purchased from LGC limited (UK) in  
271 freeze dried vials. The bacteria were cultured according to the supplier's  
272 instructions. Briefly the *P.gingivalis* FDC 381 were cultured in ATCC medium 2722,  
273 supplemented tryptic soy broth (TSB) (TSB 3%, Yeast extract 0.5%, L-cystein  
274 hydrochloride 0.05%, Hemin (5 mcg/ml) with K<sub>2</sub>HPO<sub>4</sub>, Vitamin K1 (1mcg/ml) (Sigma  
275 Aldrich, UK)) on TSA with 5% sheep blood (Thermo Scientific, UK) and FAA agar with  
276 7% horse blood Neomycin (75mg/l) (E and O, UK). All cultures were incubated at  
277 37°C in an anaerobic chamber (Bactron, USA) using an anaerobic gas mixture of 5%  
278 H<sub>2</sub>, 5% CO<sub>2</sub> and 90% N<sub>2</sub>. The cultures were grown for 3 days. The optical density (OD)  
279 of the broth cultures were measured daily and selected for use when between OD<sub>655</sub>  
280 0.1 and 1 [54]. The cultures were Gram stained and imaged for quality control daily  
281 to ensure monoculture samples utilising a Gram staining kit (Merck, UK) and inverted  
282 light microscope using a X40 and X100 objective (Leica DMIL, Germany) and a Nikon  
283 DS-L4 camera and software.

#### 284 ISOLATION OF OUTER MEMBRANE VESICLES OF P.GINGIVALIS

285 The outer membrane vesicles of *P.gingivalis* FDC 381 were isolated following the  
286 protocol used by Seyama et al. (2020)[54]. The bacterial culture in TSB was  
287 centrifuged at 2800 ×g for 15 min at 4 °C to separate the vesicles from the bacterial  
288 cells. The supernatant was passed through a 0.2 µm syringe filter (Millipore, UK) and  
289 then concentrated to under 1 mL by using an Ultra-15 Centrifugal Filter for the  
290 nominal molecular weight limit (NMWL) 100K (Sigma-Aldrich, UK). The concentrate  
291 was mixed with total exosome isolation reagent for culture (Life technologies, UK)  
292 and this was incubated at 4 °C overnight. The samples were centrifuged at 10,000 ×g  
293 for 60 min at 4 °C. The vesicles were eluted in 100 µL X1PBS. The TSB without  
294 bacteria was treated by the same method as a negative control. The diameter of the

295 outer membrane vesicles was measured and mono-dispersity ensured using a  
296 Zetasizer (Malvern Zetasizer Nano, Panalytical Instalment Ltd., UK) (55) and the  
297 concentrations of the samples was measured on the NanoDrop Spectrophotometer  
298 (280 nm) (Nanodrop 2000, Thermo Scientific, UK).

299

#### 300 BBB RESPONSE TO *P.GINGIVALIS* VIRULENCE FACTORS

301 The *in vitro* BBB model response to virulence factors of *P.gingivalis* was tested by  
302 incubations with various concentrations (0.1 µg/ml, 0.3 µg/ml, 1 µg/ml, 10 µg/ml, 50  
303 µg/ml and 100 µg/ml) of *P.gingivalis* LPS (Invivogen, France) and *P.gingivalis* outer  
304 membrane vesicles (OMV) and 1 µg/ml, 10 µg/ml, 50 µg/ml and 100 µg/ml of  
305 *P.gingivalis* LPS-FITC conjugate (Nanocs, USA). An experiment was also conducted  
306 with application of *P.gingivalis* LPS-FITC conjugate (Nanocs, USA) in combination  
307 with OMVs at 10 µg/ml. Control wells included no treatment (cell and media alone)  
308 and a cell blank (fibronectin insert, no cells). All measurements were made from  
309 each well in five times (TEER) or three times (Permeability, Papp), each plate had  
310 three wells (intraassay variability check). The test samples were diluted in complete  
311 medium of equal measures of EBM, PM and ABM. The test samples were placed in  
312 the apical compartment of the transwell and the TEER was measured at set time  
313 points (0.5,1, 2, 4, 24, 48 and 72 hours). At each time point the TEER values of the  
314 wells were measured 5 times and triplicate samples were collected from the  
315 basolateral compartment.

#### 316 APPARENT PERMEABILITY OF THE BLOOD BRAIN BARRIER TO *P.GINGIVALIS* VIRULENCE FACTORS

317 Samples from the basolateral side of the BBB model were measured in the GENios  
318 Pro plate reader (Tecan, Austria) at 490 nm excitation and 520 nm emission (gain 40,

319 22°C)[52], to quantify the appearance of fluorescent labelled LPS or FITC-dextran.  
320 The appearance from the apical to the basolateral compartment was calculated from  
321 standard curves of known concentrations of both FITC- dextran (3-5 kDa)( Sigma-  
322 Aldrich, UK) and the *P.gingivalis* LPS-FITC conjugate (Nanocs, USA) and the data  
323 from the standard curves were used to calculate the permeability (Papp) values in  
324 each experiment as shown in Equation 1.

$$325 P_{app} = \left( \frac{V}{A \times C_0} \right) \times \left( \frac{dQ}{dt} \right) \quad \text{Equation 1}$$

326 where:

327 V = Volume of basolateral compartment (V= 0.6 cm<sup>3</sup>)

328 A = surface area of the polycarbonate membrane (0.3 cm<sup>2</sup>)

329 C<sub>0</sub>= Initial concentration of the *P.gingivalis* LPS-FITC conjugate or FITC-Dextran in the  
330 apical well

331 dQ = concentration of *P.gingivalis* LPS-FITC conjugate or FITC-Dextran collected from  
332 the basolateral part (µg/ ml) (passing across the cell layer to basolateral side).

333 dt = Change in time (sec)

334

335

### 336 HUMAN IL6 ELISA

337 As a quality assurance measure to check all virulence factors (LPS, LPS-FITC  
338 conjugate and OMVs) were capable of producing an inflammatory response, all test  
339 reagents were evaluated for inflammasome activity by incubation (100 µg/ml) with  
340 HBVP for 4 hours in triplicate and the spent cell culture media was assayed for

341 human IL-6 release using a commercially available enzyme-linked immunosorbent  
342 assay (ELISA) kit (Sigma-Aldrich, USA). Test samples (spent media), controls (sample  
343 diluent buffer) and human IL-6 standards (100 µL) were added to the precoated 96  
344 well ELISA plate. This was incubated at 4 °C for 24 hours with gentle shaking. After  
345 removal of the samples the wells washed with X1 wash buffer four times.  
346 Biotinylated detection antibody was added and incubated for 1 hour at room  
347 temperature with gentle shaking. The wells were washed four times with X1 wash  
348 buffer and HRP- streptavidin solution was incubated for 45 minutes at room  
349 temperature with gentle shaking. After washing four times with X1 wash buffer,  
350 ELISA colorimetric TMB reagent was added. This was incubated for 30 minutes at  
351 room temperature covered to exclude light while gently shaking. Then stop solution  
352 was added and the absorbance was measured in the 96-well plate immediately at  
353 450 nm (Tecan, Austria). A standard curve was produced, the concentration of IL-6 in  
354 the samples was calculated.

355 IMMUNOFLUORESCENT IMAGING OF P.GINGIVALIS VIRULENCE FACTORS INTERACTIONS WITH TIGHT

356 JUNCTION PROTEINS OF HBMEC CELLS

357 HBMECs (Neuromics, USA) were seeded at a density of 250000 cells/ml in black,  
358 tissue culture treated 24-well µ-plates (IBIDI at Thistle scientific, UK) and grown in  
359 EBM (Lonza, Switzerland) in a 37 °C humidified incubator under 5 % CO<sub>2</sub> for 8 days.  
360 The cells were tested for viability with Trypan Blue (Sigma-Aldrich, UK) and by visual  
361 daily inspection. On day 7 the cells were treated with 0.1 µg/ml and 0.3 µg/ml of  
362 unconjugated *P.gingivalis* LPS (Invivogen, France) or *P.gingivalis* outer membrane  
363 vesicles (OMV) diluted in EBM (Lonza, Switzerland) and incubated for 24 hours. After  
364 this incubation period the cells were fixed for IF protocol described below.



365 After incubation with the test samples the cells were washed in x1 PBS and fixed  
366 with 4% formaldehyde, washed and permeabilised with x1 PBS and 0.1% Triton-X  
367 (Sigma- Aldrich, UK) and blocked with 20 % normal goat serum (Stratech, UK) in 1x  
368 PBS with 0.1% Triton-X for 60 minutes. The cells were incubated with the primary  
369 antibody ZO-1 (D6L1E) Rabbit mAb (1:400) (Cell signalling, NL) at 4°C for 12 hours  
370 and shaking and the secondary antibody Cy™5 AffiniPure Goat Anti-Rabbit IgG  
371 (1:800) (Jackson Immuno, USA) for an hour at 4°C. The cells were counter stained with  
372 DAPI(1:3500) (Stratech, UK) and imaged in a Zeiss Cell Observer system featuring the  
373 Zeiss definite focus, Colibri LED illumination and AxioVision 4 digital image  
374 processing software (Carl Zeiss Microscopy, Germany) detecting the signal for DAPI  
375 at ex:358 nm em:463 nm and Cy5 ex:646 nm em:664 nm. The images were viewed  
376 and processed using Zen 2.3 Lite software.

## 377 STATISTICAL ANALYSIS

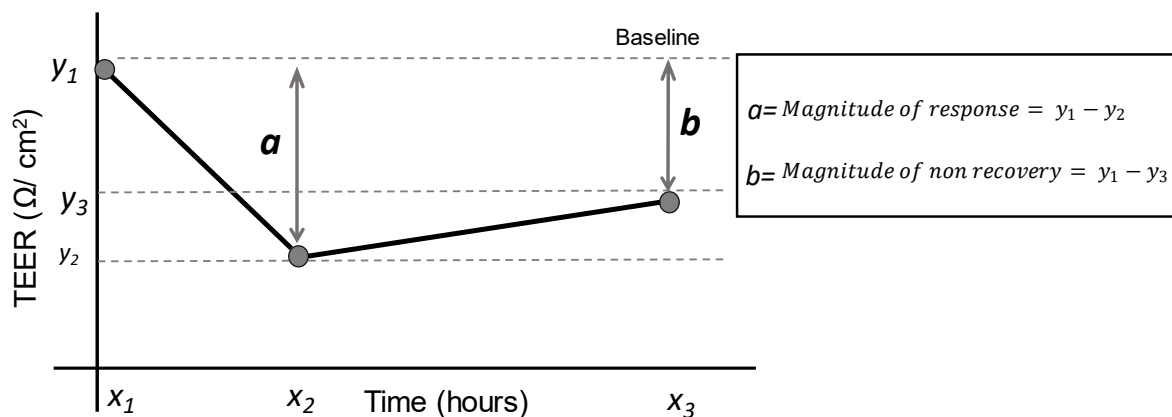
378 The TEER and the permeability (Papp) data obtained from the *in vitro* BBB model was  
379 tested for homogeneity of variances and normality using the Shapiro-Wilk test.  
380 Difference between treatment groups was analysed using an ANOVA with Dunnett's  
381 post-hoc analysis or an independent t-test for comparison between independent  
382 experiments. The analysis was performed using the Statistical Package SPSS Version  
383 26 and 27 (IBM, USA). Statistical significance was defined when (\*)  $P < 0.05$ , and  
384 highly significant when (\*\*)  $P < 0.01$  and (\*\*\*)  $P < 0.001$ .

385

## 386 RESULTS

### 387 BASELINE VARIABILITY AND MODELLING TEER CHANGES IN THE BBB MODEL

388 The baseline of the experimental model and optimisation was carried out to  
 389 establish whether the primary cells and the 3-layer model were suitable for the  
 390 planned experiments and not affected by the presence of the tracer compound.  
 391 Prior to the start of the experiment, TEER values were consistent from day 7, with a  
 392 typical variation of  $\pm 10 \Omega/\text{cm}^2$  over a 4 hour time period. Upon addition of either  
 393 unconjugated *P.gingivalis* LPS (test wells), media (blank wells) or FITC (control wells)  
 394 to the apical side of the BBB, there was a small initial dip in TEER at the start of the  
 395 experiment that was attributable to movement artefact and slight disturbance of the  
 396 BBB in all wells, typically this was  $\pm 25 \Omega/\text{cm}^2$  and recovery to baseline was observed  
 397 in the control wells within 2 hours. The response of TEER in test wells upon addition  
 398 of unconjugated LPS often showed a lower drop in TEER and that did not always  
 399 recover to pre-baseline TEER. To determine whether the change in TEER was  
 400 significantly different from baseline variation or movement artefacts, the pattern of  
 401 response was modelled and the magnitude ( $\Delta\text{TEER}$ ), recovery time and rate of  
 402 change were defined as shown in Figure 1 and were then used for statistical  
 403 comparison between the control and test wells at different LPS concentrations.  
 404



405  
 406 *Figure 1. Modelling the magnitude and rate of change in TEER after application of*

407 *test sample to the in vitro BBB model*

408

409 CONFIRMATION OF INFLAMMATORY RESPONSE OF VIRULENCE FACTORS TESTED, MEASURED BY

410 HUMAN IL6 ELISA

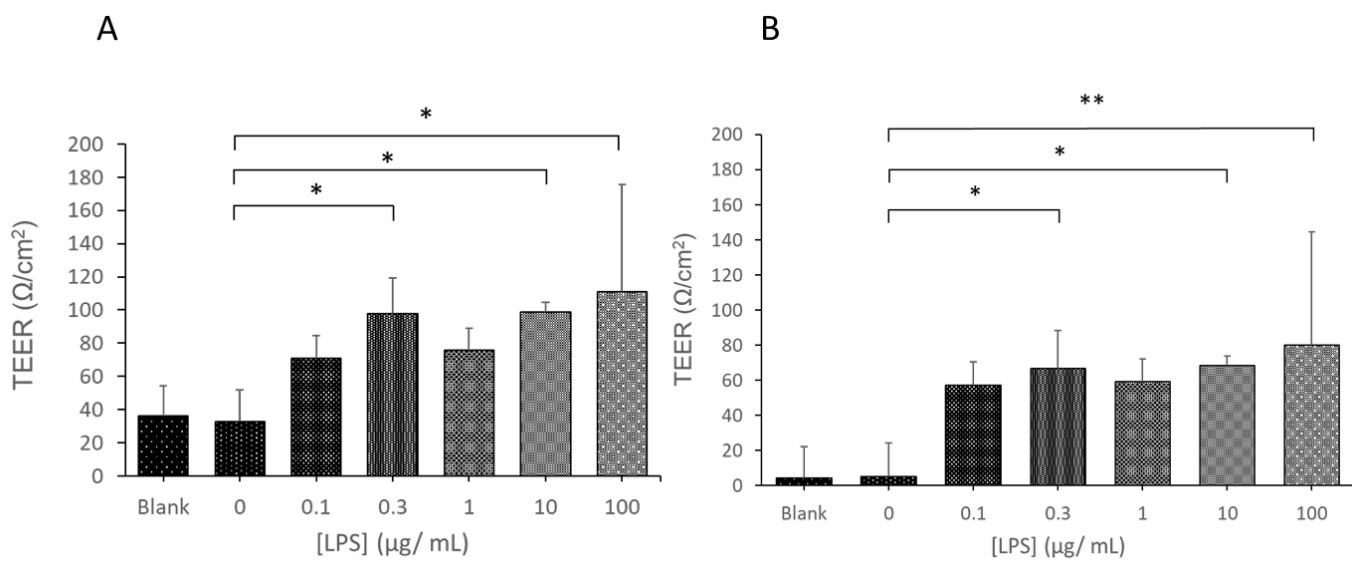
411 In order to show that the virulence factors applied to the BBB model (unconjugated  
412 *P.gingivalis* LPS, FITC *P.gingivalis* LPS and *P.gingivalis* OMVs) had a biological  
413 response all samples were tested for induction of IL6 in HBPC prior to use. The  
414 inflammatory response of HBPC cells following exposure to unconjugated  
415 *P.gingivalis* LPS, FITC *P.gingivalis* LPS conjugated and *P.gingivalis* OMVs (all 100  
416 µg/ml) after 4 hours of co-incubation, negative controls were media only. A standard  
417 curve was prepared and used to determine the concentrations of IL6 secreted by the  
418 cells in the test wells. This test was repeated every time a new conjugate reagent  
419 was used for the first time in triplicates. The results showed an elevated level of IL6  
420 in the test samples compared to controls (data not shown). These results were seen  
421 as a positive control of the virulence activity in the samples tested.

422

423 EFFECT OF UNCONJUGATED P.GINGIVALIS LPS ON THE BBB INTEGRITY

424 The *in vitro* model was tested with un conjugated *P.gingivalis* LPS to assess the  
425 barrier response to this virulence factor. Application of unconjugated *P.gingivalis*.  
426 LPS to the BBB caused a significant decrease in TEER for 0.3 µg/ml ( $P \leq 0.05$ ), 10  
427 µg/ml ( $P \leq 0.05$ ) and 100 µg/ml ( $P \leq 0.05$ ) when compared the magnitude of change  
428 to the control well, where FITC alone or media alone were administered (Figure 2A).  
429 The magnitude of recovery of TEER values determined as the maximum TEER  
430 measured during the recovery phase. For all wells treated with unconjugated

431 *P.gingivalis* LPS there was still a deficit in recovery of the BBB integrity compared to  
 432 the pre-incubation phase, as indicated by the deficit in TEER 72 hours post  
 433 incubation relative to the baseline at time zero. The magnitude of deficit in TEER was  
 434 significantly greater in the test wells where unconjugated *P.gingivalis* LPS was  
 435 applied at 0.3 µg/ml ( $P \leq 0.05$ ), 10 µg/ml ( $P \leq 0.05$ ) and highly significant with 100  
 436 µg/ml ( $P \leq 0.01$ ) compared to the control wells where FITC-alone was applied to the  
 437 BBB (Figure 2B).

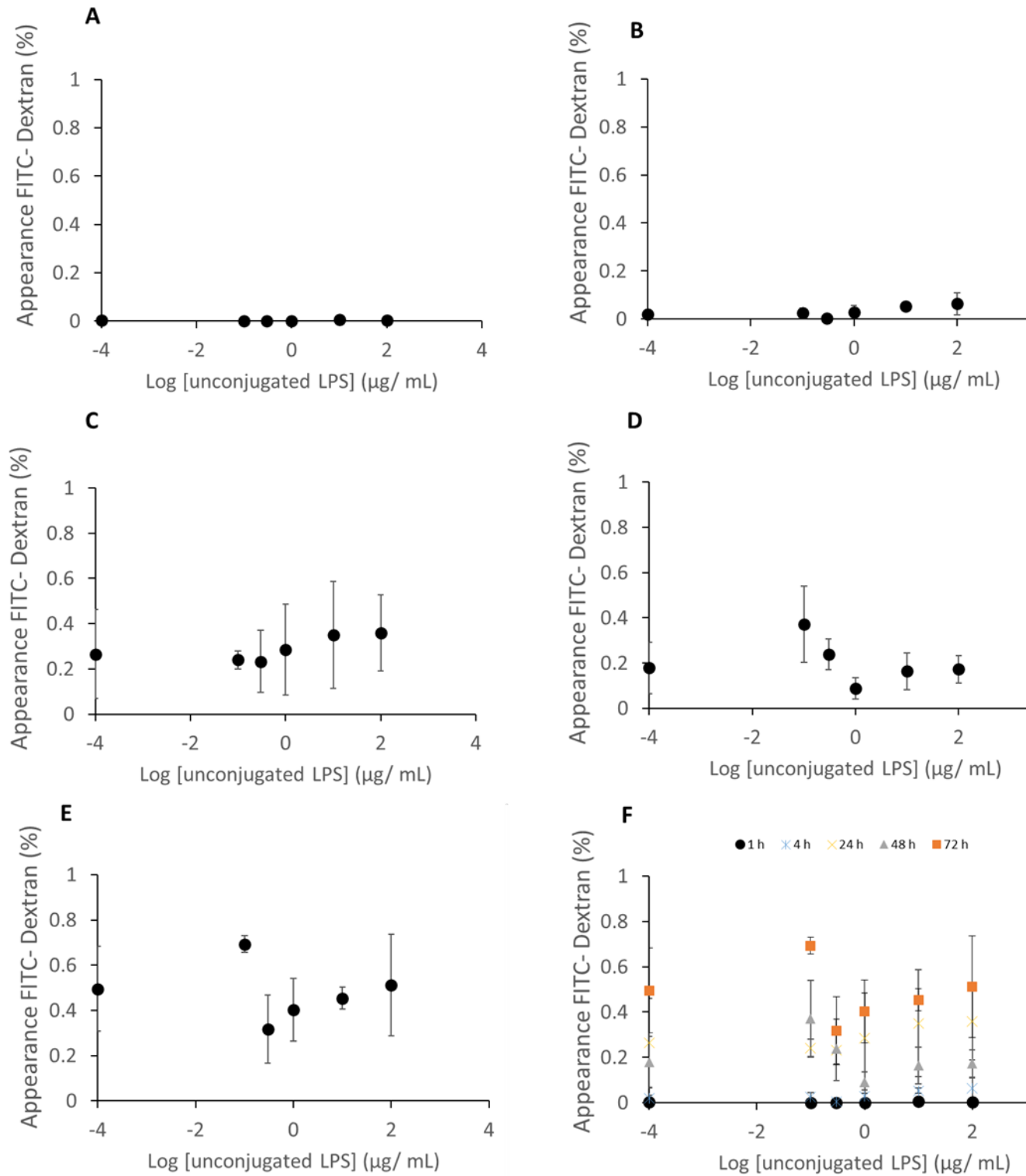


438  
 439 *Figure 2 Changes in BBB integrity measured by calculating the magnitude of decrease*  
 440 *in TEER in response to application of unconjugated P.gingivalis LPS (A) and the*  
 441 *magnitude of deficit in recovery of TEER 72 hours post application of unconjugated*  
 442 *P.gingivalis LPS relative to initial baseline TEER (B). Statistical significance of response*  
 443 *was measured using an ANOVA with Dunnett's post-hoc relative to the control*  
 444 *(administration of FITC alone) where \* $P < 0.05$  and \*\* $P < 0.01$ . Data represents mean  $\pm$*   
 445 *SD from three wells and two experimental repeats (n=6).*

446  
 447 The integrity of the *in vitro* BBB model was also assessed by testing the wells with  
 448 FITC-Dextran 3-5 kD as a marker of tight junction permeability. After incubation with  
 449 unconjugated *P.gingivalis*. LPS or media (blank) for set time points. FITC-Dextran 3-5  
 450 kD was added to the wells and the fluorescent appearance of FITC-dextran on the  
 451 basolateral side of the BBB was measured. It was observed that the FITC-Dextran

452 appeared earlier in the wells with 10 and 100 µg/ml of unconjugated *P.gingivalis* LPS  
453 following pre-incubation however this was not statistically significant relative to the  
454 blank wells and no significant concentration dependent effect in *P.gingivalis* LPS  
455 treatment related to FITC-dextran appearance was observed for the complete test  
456 period. The percentage appearance of FITC-dextran appeared to increase following  
457 longer exposure (24-72 hours) to *P.gingivalis* LPS, as shown in Figure 3C-E.

458



459

460

461

462

463

464

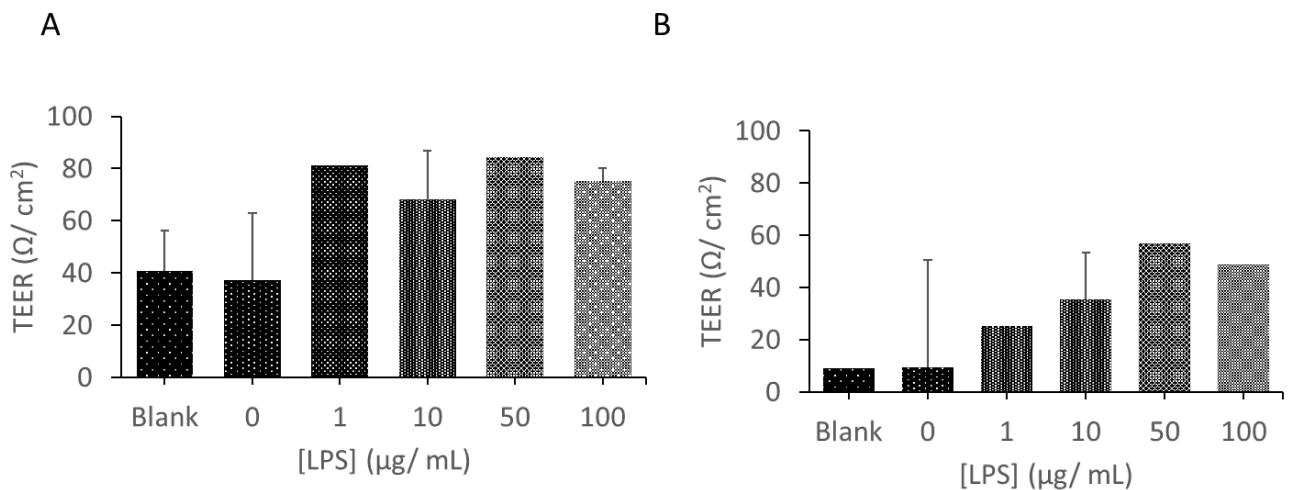
465

Figure 3. Shows the percentage of FITC-dextran (3-5 kDa) permeating through the in vitro BBB after incubation with increasing concentrations of unconjugated P.g. LPS (0-100 µg/ mL) for 1 h (A); 4 h (B); 24 h (C); 48 h (D); 72 h (E) and all exposure times compared together (F). Each data point represents mean  $\pm$  SD from three wells and two experimental repeats (n=6).

466 The apparent permeability (Papp) of FITC-dextran (100 µg/ mL) after incubation for  
467 30 minutes was calculated for three time points (60, 120 and 240 minutes) as  
468 described previously. Final Papp values at 60 min, 120 min and 240 min were found  
469 to be  $1.04 \times 10^{-8} \pm 2.3 \times 10^{-8}$  cm/s,  $8.7 \times 10^{-8} \pm 1.7 \times 10^{-7}$  cm/s and  $4.8 \times 10^{-8} \pm 4.7$   
470  $\times 10^{-8}$  cm/s.

471 EFFECT OF FITC-CONJUGATED P.GINGIVALIS LPS ON THE BBB INTEGRITY

472 To investigate potential transport across the *in vitro* BBB model a FITC labelled  
473 *P.gingivalis* LPS was applied to the established model and appearance of the  
474 conjugate was measured with the models integrity. It was shown that there were no  
475 significant differences in the magnitude of TEER response between the wells with  
476 application of all concentrations of FITC-*P.gingivalis* LPS conjugate and the control  
477 (FITC alone), however a decrease in TEER was observed in all wells after application  
478 of 1,10,50 and 100 µg/ml (Figure 4A). These wells did not appear to recover as well  
479 compared to controls (Figure 4B).



480  
481 *Figure 4 Changes in BBB integrity measured by calculating the magnitude of decrease*  
482 *in TEER in response to application of conjugated FITC-P.gingivalis LPS (A) and the*  
483 *magnitude of deficit in recovery of TEER 72 hours post application of conjugated*  
484 *FITC-P.gingivalis LPS relative to initial baseline TEER (B).No statistical significance of*  
485 *response was measured using an ANOVA with Dunnett's post-hoc relative to the*

486 *control (administration of FITC alone). Data represents mean  $\pm$  SD from three wells*  
487 *and two experimental repeats (n=6).*

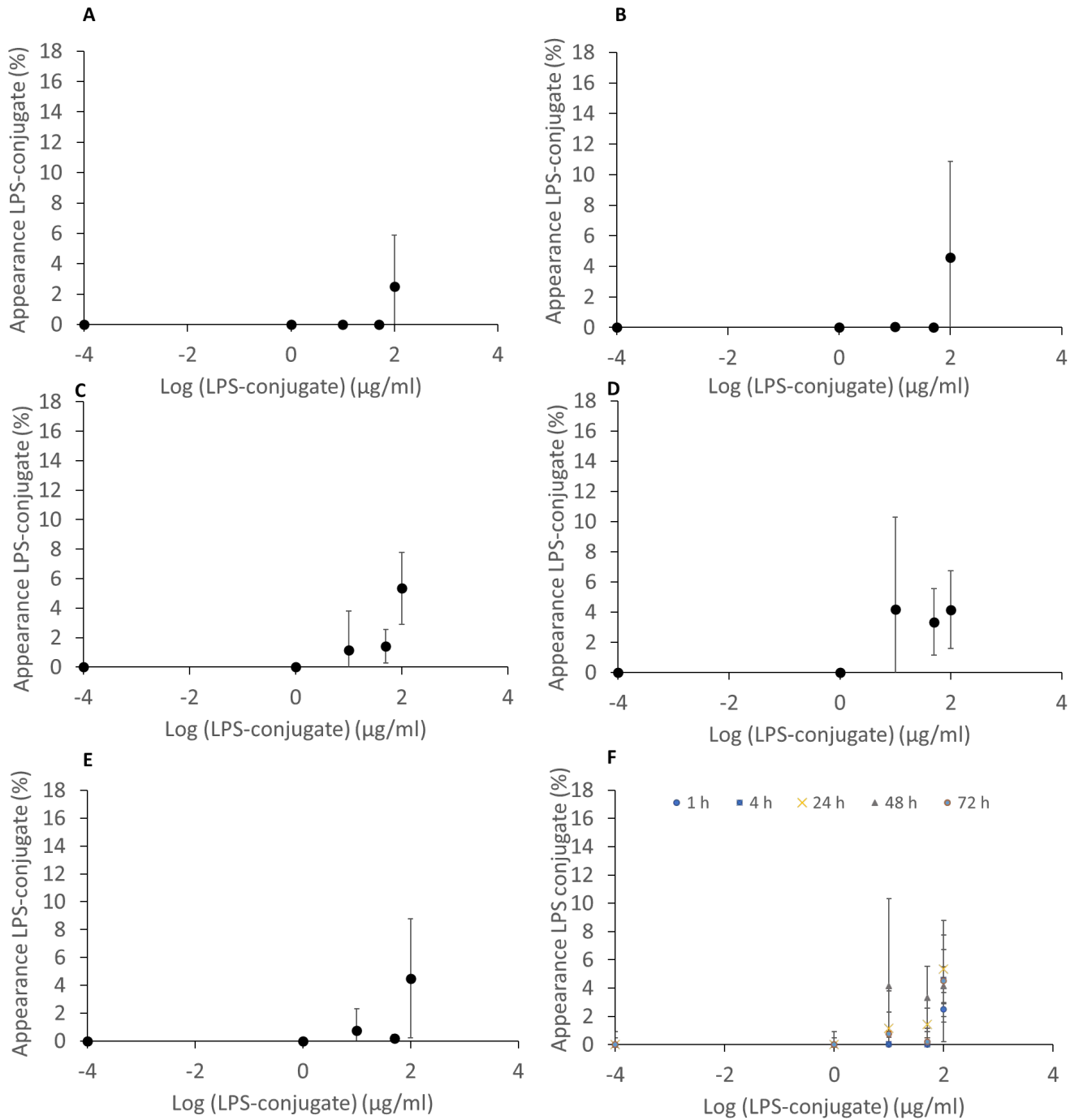
488

489 The appearance of the FITC *P.gingivalis* LPS was greatest in the highest  
490 concentration (100 $\mu$ g/ml) at 1 and 4 hours (Figure 5A and 5B) and an increase of  
491 percentage appearance was observed with the concentrations 10 and 50  $\mu$ g/ml as  
492 the experiment progressed at 24 and 48 hours (Figure 5C and 5D). The percentage  
493 appearance of the FITC *P.gingivalis* LPS in the basolateral compartment of the model  
494 did not exceed 5% during the duration of the experiments. A drop in the TEER values  
495 were seen to correlate with the appearance of the conjugate in all the wells of the  
496 higher concentrations (50  $\mu$ g/ml and 100  $\mu$ g/ml LPS) (data not shown).  
497 All the wells were tested with FITC-Dextran at the end of each experiment to assess  
498 the final integrity of the barrier (data not shown).

499

500





501

502

503

504

505

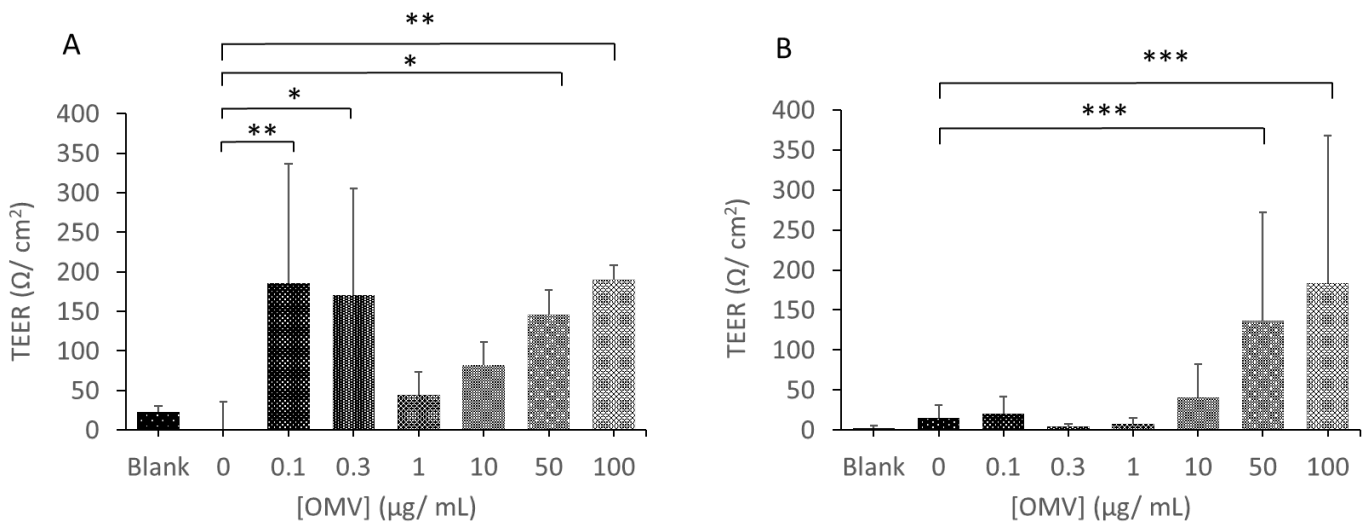
506

Figure 5 Percentage appearance of FITC *P.gingivalis* LPS conjugate on the apical side of the *in vitro* BBB model relative to the stock FITC *P.gingivalis* LPS administered to the basolateral side after 1 h (A); 4 h (B); 24 h (C); 48 h (D); 72 (E) and a comparison of all time points (E). Statistical significance of response was measured using an ANOVA with Dunnett's post-hoc relative to the control (administration of FITC alone)

507 where \* $P < 0.05$  and \*\* $P < 0.01$ . Data represents mean  $\pm$  SD from three wells and two  
 508 experimental repeats ( $n=6$ ).

509 EFFECT OF *P. GINGIVALIS* OMVS ON THE BBB INTEGRITY

510 The application of *P.gingivalis* OMVs showed similar patterns to the LPS study. The  
 511 magnitude of decrease in TEER observed in response to treatment with OMVs was  
 512 significantly different from the control group for the 0.1  $\mu\text{L}/\text{mL}$  ( $P < 0.01$ ); 0.3  $\mu\text{L}/\text{mL}$   
 513 ( $P < 0.05$ ); 50  $\mu\text{L}/\text{mL}$  ( $P < 0.05$ ) and 100  $\mu\text{L}/\text{mL}$  ( $P < 0.01$ ) (Figure 6A). This decrease in  
 514 TEER did not recover to pre-treatment baseline for the wells treated with 50 and 100  
 515  $\mu\text{L}/\text{mL}$  *P.g* OMVs as the magnitude of deficit was highly significantly different to the  
 516 control group ( $P < 0.001$ ), as shown in Figure 6B.



517  
 518 *Figure 6 Changes in BBB integrity measured by calculating the magnitude of*  
 519 *decrease in TEER in response to application of *P.gingivalis* OMVs (A) and the*  
 520 *magnitude of deficit in recovery of TEER 72 h post application of conjugated*  
 521 **P.gingivalis* OMVs relative to initial baseline TEER (B). Statistical significance of*  
 522 *response was measured using an ANOVA with Dunnett's post-hoc relative to the*  
 523 *control (administration of FITC alone) where \* $P < 0.05$ , \*\* $P < 0.01$  and \*\*\* $P$*   
 524  *$< 0.001$ . Data represents mean  $\pm$  SD from three wells and two experimental repeats*  
 525 *( $n=6$ ).*

526

527 Figure 7 shows the appearance of FITC-Dextran permeation following incubation of  
528 the *in vitro* BBB with increasing concentrations of *P.gingivalis*. OMV exposed for  
529 varying durations. Similar to the unconjugated LPS, the effect of OMV treatment on  
530 the extent of FITC-dextran permeation was fairly constant after the 12 hour  
531 exposure, but this time the permeation did appear to increase as the concentration  
532 of OMV increased (Figure 7C-E).

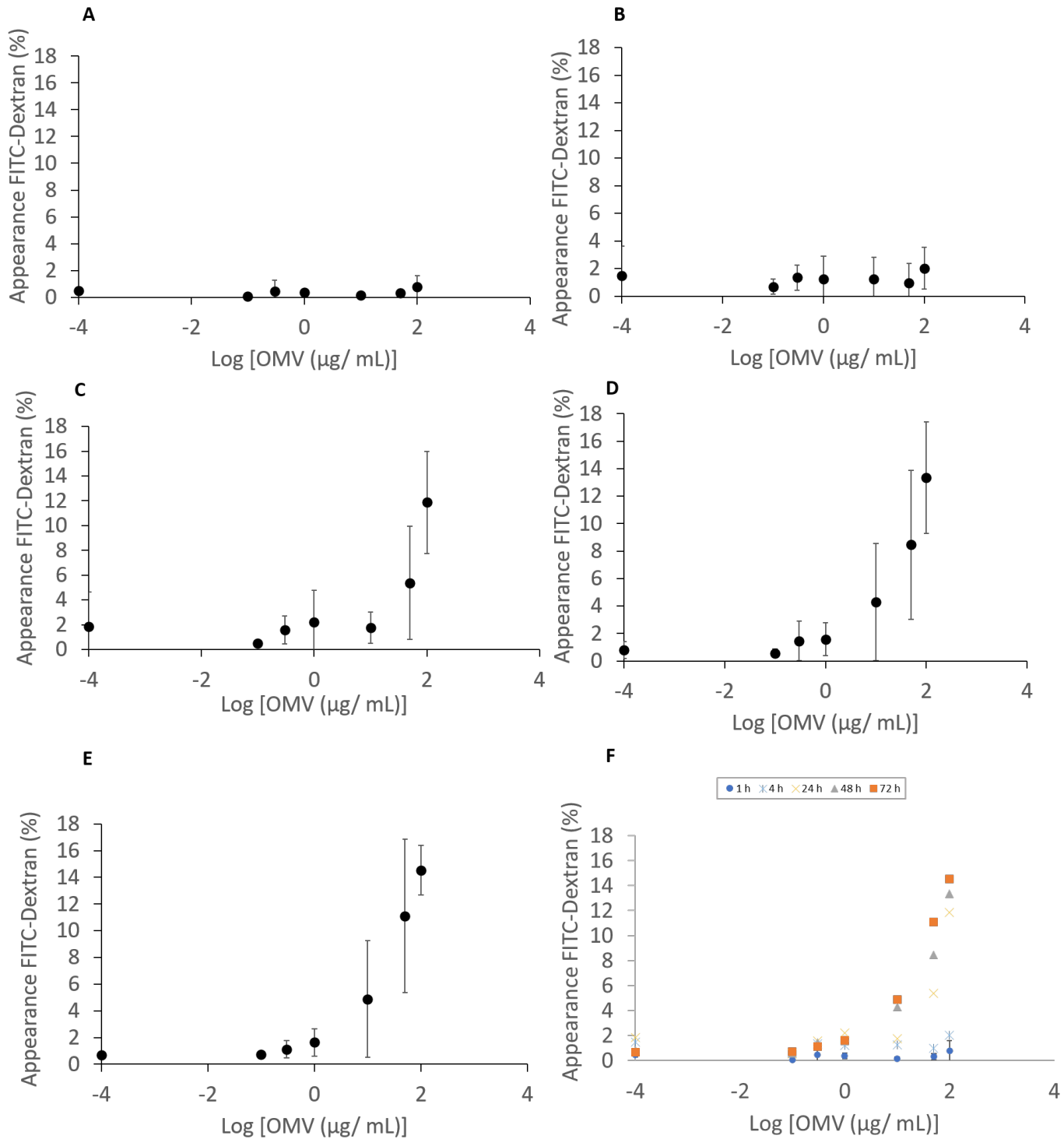
533

534

535

536

537



538

539

540

541

542

543

544

545

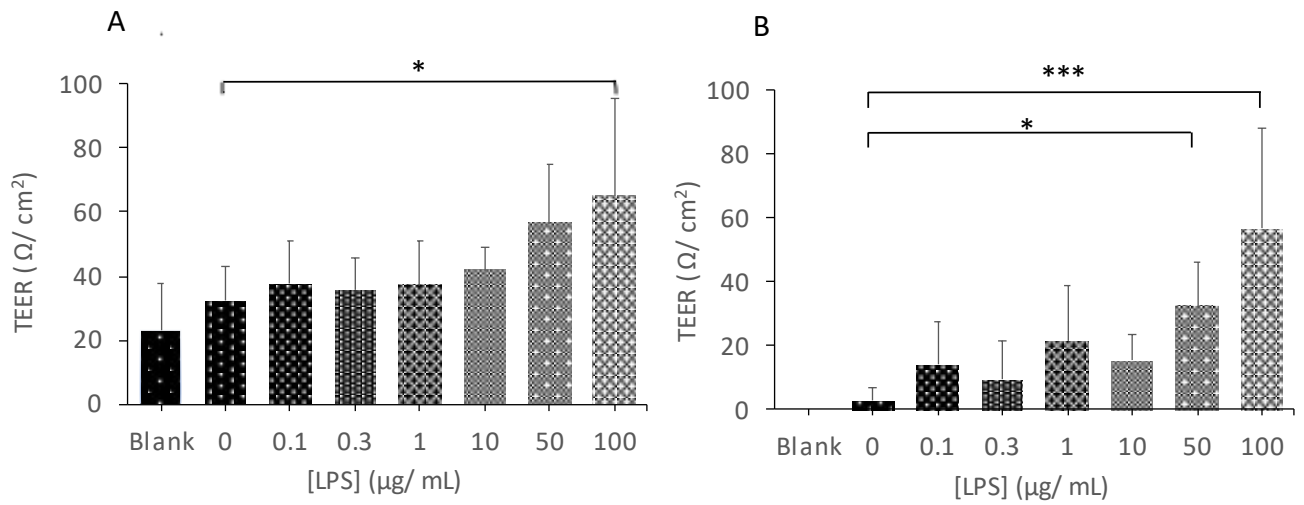
546

Figure 7 Percentage appearance of FITC-dextran (3-5 kDa) on the apical side of the in vitro BBB model after application of *P.gingivalis* OMVs, percentage appearance relative to the stock FITC-dextran administered to the basolateral side after 1 h (A); 4 h (B); 24 h (C); 48 h (D); 72 (E) and a comparison of all time points (E). Statistical significance of response was measured using an ANOVA with Dunnett's post-hoc relative to the control (administration of FITC alone) where \* $P < 0.05$  and \*\* $P < 0.01$ . Data represents mean  $\pm$  SD from three wells and two experimental repeats ( $n=6$ ).

547 EFFECT OF *P.GINGIVALIS* OMV AND LPS ON THE BBB INTEGRITY

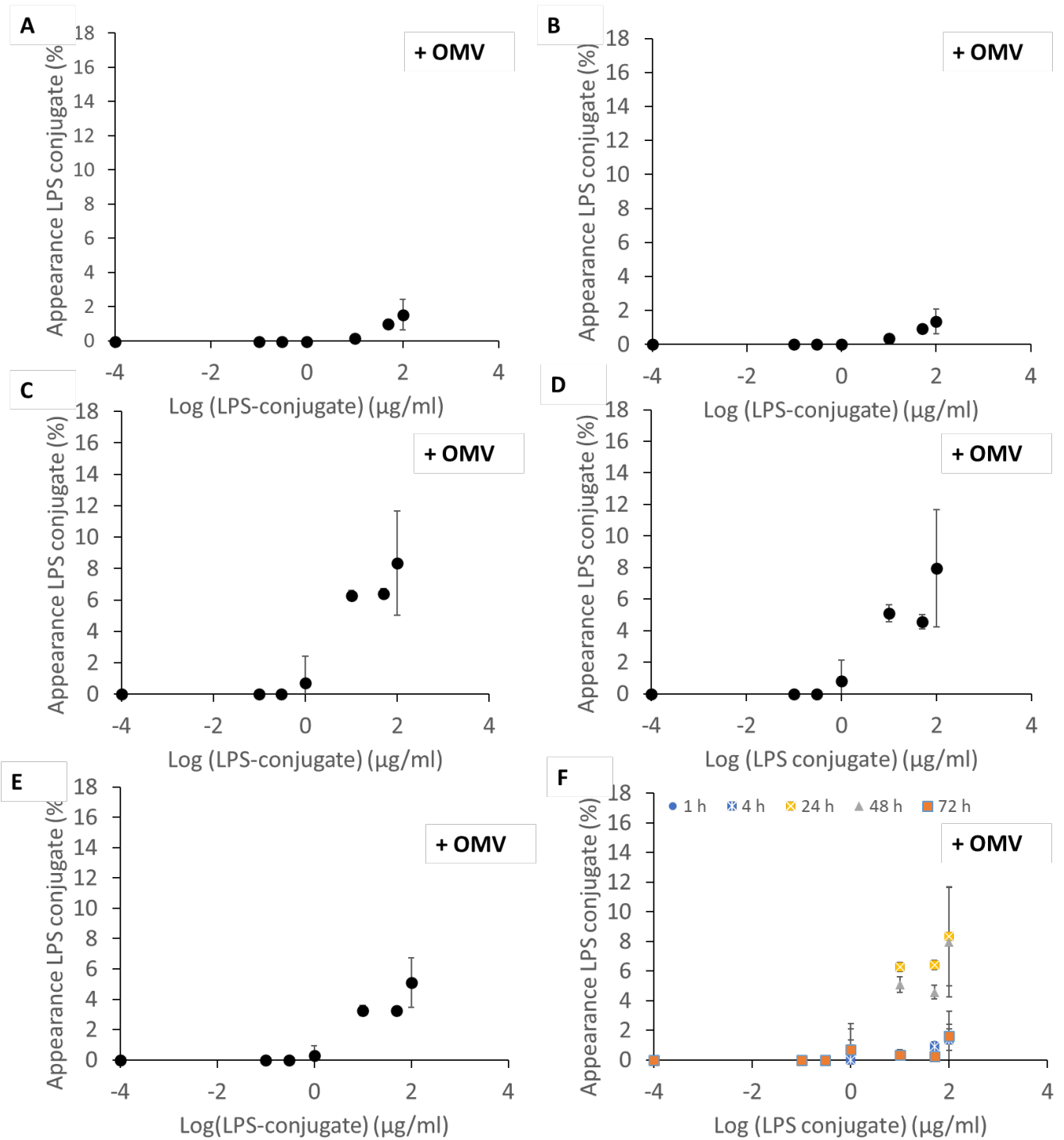
548 The *in vitro* BBB model was tested with FITC conjugated *P.gingivalis* LPS in the  
549 presence of a constant concentration of OMV to assess the effect the OMVs could  
550 potentially have on the appearance of the conjugated LPS in the basolateral  
551 compartment. The concentration of OMV was chosen (10 µg/ml) as this was the  
552 lowest which showed an effect in the BBB models integrity in the OMV only  
553 experiment previously (Figure 7D). The controls for the combined experiment were  
554 media only and OMV (10 µg/ml) only. The data was compared to the previous  
555 experiments with FITC *P.gingivalis* LPS only (Figure 5). The application of *P.gingivalis*  
556 LPS-FITC conjugate in conjunction with 10 µg/ml *P.gingivalis* OMVs showed a similar  
557 pattern in terms of response in the BBB model as seen in the previous experiments.  
558 The TEER responses in these experiments showed a significant difference in the  
559 100µg/mL FITC *P.gingivalis* LPS conjugate with larger magnitudes of change in TEER  
560 compared to the controls (P<0.05) (Figure 8A). The higher the concentration of FITC  
561 *P.gingivalis* LPS with OMV, a reduced recovery was observed, although this was only  
562 significant in the highest concentration of 50 µg/mL and highly significant in the  
563 100µg/mL FITC *P.gingivalis* LPS with 10 µg/ml OMVs ((P<0.05 and (P<0.001)) (figure  
564 8B). An increase in the permeability was seen especially after 24 hours where some  
565 of the increases were 5-fold compared to the experiment with *P.gingivalis* LPS-FITC  
566 conjugate application only, though this increase was not significant (Figures 5 and  
567 9C).

568



570 *Figure 8 Changes in BBB integrity measured by calculating the magnitude of decrease*  
 571 *in TEER in response to application of FITC P.gingivalis LPS conjugate and 10 μg/ml*  
 572 *P.gingivalis OMVs (A) and the magnitude of deficit in recovery of TEER 72 hours post*  
 573 *application of of FITC P.gingivalis LPS conjugate and 10 μg/ml P.gingivalis OMVs*  
 574 *relative to initial baseline TEER (B). Statistical significance of response was measured*  
 575 *using an ANOVA with Dunnett’s post-hoc relative to the control (administration of*  
 576 *FITC alone) where \*P<0.05 and \*\*\*P <0.001. Data represents mean ± SD from three*  
 577 *wells and two experimental repeats (n=6).*

578



579

580

581

582

583

584

585

586

587

Figure 9 Percentage appearance of FITC *P.gingivalis* LPS conjugate on the basolateral side of the *in vitro* BBB model relative to the stock administered to the apical side after 1 h (A); 4 h (B); 24 h (C); 48 h (D); 72 (E) and a comparison of all time points (E). Statistical significance of response was measured using an ANOVA with Dunnett's post-hoc relative to the control (administration of FITC alone) where \* $P < 0.05$  and \*\* $P < 0.01$ . Data represents mean  $\pm$  SD from three wells and two experimental repeats ( $n=6$ ).

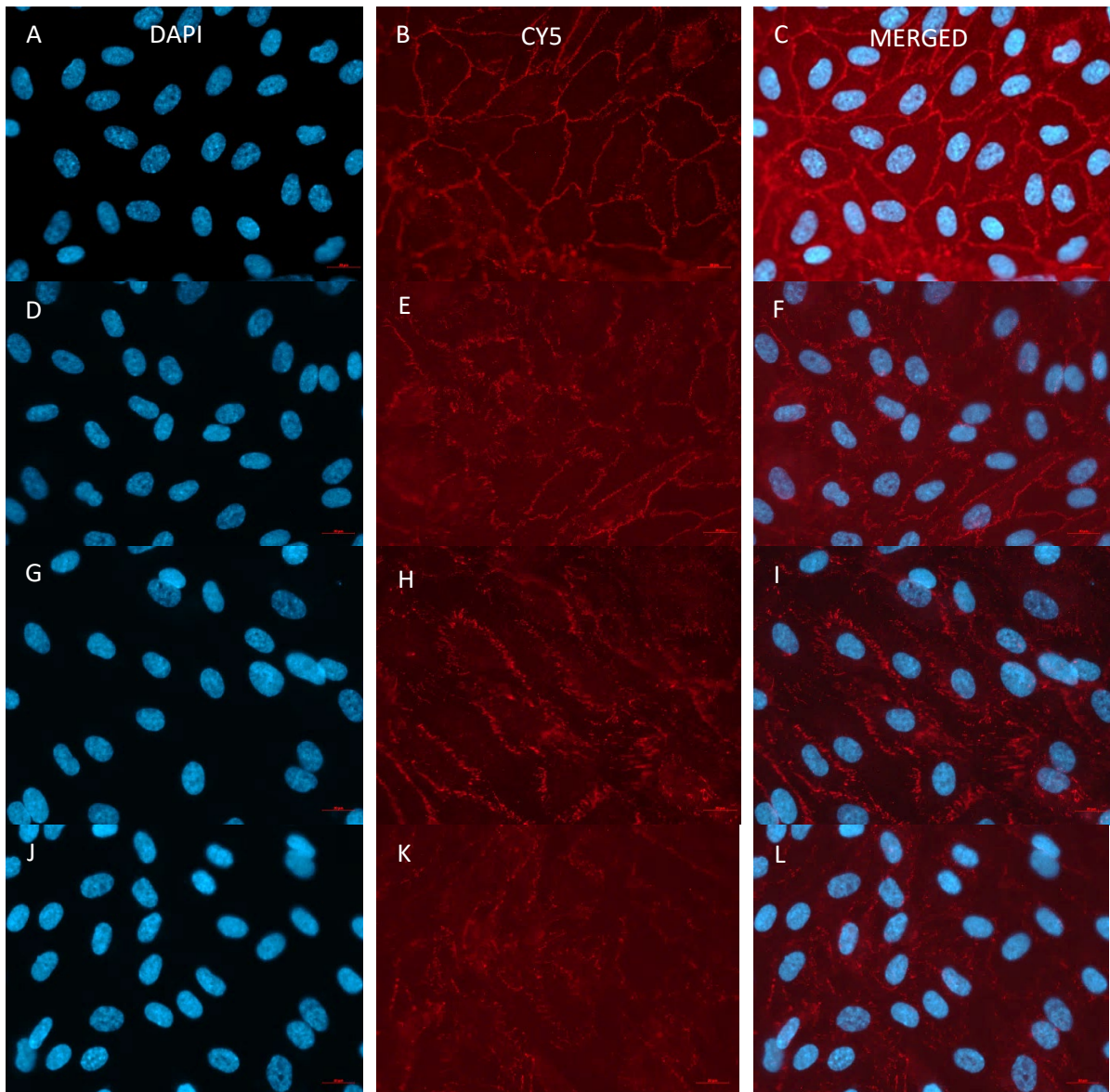
588 ASSESSMENT OF VIRULENCE FACTORS INTERACTIONS WITH HBMEC MONOLAYERS MEASURED BY  
589 IMMUNOFLUORESCENCE MICROSCOPY

590 The experiments of application of virulence factors to the BBB model indicated a  
591 potential disruption of the barrier. These findings lead to the experiment with  
592 application of i) unconjugated *P.gingivalis* LPS (0.1 and 0.3 µg/ml) and ii) OMVs (0.1  
593 and 0.3 µg/ml) to HBMEC cells in monolayer with an aim to determine how the  
594 observed BBB model disruption happened, all the experiments were repeated 3  
595 times independently. The HBMEC cells were chosen for this experiment as these are  
596 the first cells coming into contact with the virulence factors in the *in vitro* model. The  
597 negative control cells (no virulence factors applied) showed the expected position of  
598 the ZO-1 protein at the cell-cell junctions and the signal of the ZO-1 protein  
599 appeared clear and well organised in these controls (Figure 10B and 10C). The  
600 concentrations for these experiments were based on observations after application  
601 of virulence factors of higher concentrations in the optimisation stages showed the  
602 HBMEC cells viability were consistently acceptable at these concentrations. All the  
603 test wells and controls were imaged using the same exposure times and all post  
604 exposure modifications were carried out to the same level with the Zen software.  
605 The HBMEC monolayer with application of *P.gingivalis* LPS showed no noticeable  
606 effect on the ZO-1 signal (Figure 10 D-F) (only 0.3 µg/ml shown) and similar  
607 observations were made in the wells with 0.1 µg/ml *P.gingivalis* OMV application  
608 (Figure 10 G-I) compared to the untreated controls (media only). The wells with  
609 application of 0.3 µg/ml *P.gingivalis* OMVs showed a more diffused signal from the  
610 ZO-1 proteins compared to untreated controls, which could appear as a reduction in  
611 the signal (Figure 10 J-L) though a change in the signal from the application of 0.3  
612 µg/ml *P.gingivalis* OMVs were seen in all 3 repeat experiments it was not clear if the  
613 change was a displacement of the ZO-1 protein or reduced numbers as the



614 experiment here did not quantify the protein. All experiments were conducted with  
615 controls both for treatments, antibodies and counterstains and all showed the  
616 correct results.

617  
618  
619  
620



621  
622 *Figure 10. Immunofluorescent study of application of P.gingivalis virulence factors to*  
623 *HBMEC cells. HBMEC cells in monolayer were treated with EBM (A-C), 0.3 µg/ml*  
624 *P.gingivalis LPS (D-F), 0.1 µg/ml P.gingivalis OMVs (G-I) or 0.3 µg/ml P.gingivalis*

625 OMVs (J-L) for 24 hours. Panels A, D, G and J show the nuclei stained with DAPI and  
626 detected at 358 nm (blue). Panels B, E, H and K show Cy5 signal detected at 646 nm  
627 (red) detecting the primary ZO-1 (D6L1E) Rabbit mAb. Panels C, F, I and L represent  
628 the composite pictures. Images were taken with 60x objective oil lens with the same  
629 exposure times. Scale bar 20  $\mu\text{m}$ . (For interpretation of the reference to colour in this  
630 figure legend, the reader is referred to the article).

631

632

### 633 DISCUSSION

634 In this study we investigated the effect of *P.gingivalis* virulence factors on the cells in  
635 a human *in vitro* BBB model. Our observations regarding the movement of  
636 *P.gingivalis* LPS across to the CNS side of the model (Figure 5) and the enhancement  
637 of LPS appearance in the basolateral compartment in the presence of OMVs (Figure  
638 9), supports findings from animal and other *in vitro* studies [17,19,20,27], though the  
639 methodology used in this study has not, to our knowledge been previously  
640 published. Designing robust human studies of chronic bacterial interaction at the  
641 BBB is challenging and making a link to sporadic AD must be carried out cautiously  
642 for numerous reasons, such as the latent period before AD pathological changes are  
643 first identified in brain tissues, and time to clinical symptomatology development  
644 both in the arena of multiple other risk factors associated with AD development. *In*  
645 *vitro* BBB models have been widely used for decades to investigate drug transport  
646 and individual disease processes, including A $\beta$  clearance mechanisms in relation to  
647 AD [49,56]. Most BBB model studies investigating bacterial related interactions have  
648 focused on acute events [57,58].

649 The *in vitro* BBB model utilised in this study was developed by Kumar et al.  
650 (2014)[50] and subsequently validated for investigation of drug transportation across

651 the BBB . Although the main protocols for the model were established, some  
652 adjustments had to be made for it to be meaningful in our investigation. It was vital  
653 to establish continuous barrier integrity or function and to ensure the model was  
654 suitable for the duration of testing and not affected by the application of FITC tracer  
655 compounds. The concentrations of virulence factors applied were deduced from  
656 previous studies [7,59] and by optimising the test protocols for which both high and  
657 low doses were included. Starting with low concentrations, the virulence factors  
658 assessment evidenced whether there was a concentration dependent relationship  
659 with the endotoxin and OMVs which would indicate the resilience of the BBB model  
660 to these virulence factors. After application of unconjugated *P.gingivalis* LPS, a clear  
661 pattern emerged (Figure 1), of an initial drop in TEER values including the controls,  
662 but it was observed that the drop in the wells which had endotoxin applied were  
663 both greater in values and failed to recover as well as those in the control wells  
664 indicating a lasting measurable effect in the BBB model barrier function. It was  
665 concluded that the initial small drop in TEER values in the control wells (average of  
666 25 ohms/cm<sup>2</sup>) would need to be regarded as an artefact and test results within these  
667 ranges were reviewed taking this into consideration by ensuring appropriate blank  
668 (media only) and zero controls (FITC only) were included in every experiment where  
669 appropriate. This artifact was not observed by Kumar et al. (2014) because the  
670 protocols utilised here included continuously measuring of the TEER levels  
671 throughout the experiments, whereas Kumar et al. used TEER as a quality control of  
672 the barrier function before and after the experimental drug transport protocols.  
673 This artifact can be explained as following the application of the Evom electrodes or  
674 the media change, a short-lived disturbance could have occurred in the conductance  
675 across the BBB model. This initial drop recovered in all the control wells and as the  
676 protocol continued for 72 hours, a clear distinction between the test and control

677 wells was facilitated (data not shown).

678 A significant drop in TEER values was seen in wells tested with the concentrations of  
679 unconjugated *P.gingivalis* LPS (0.3, 10, 100µg/ml) (Figure 2A) and the recovery of  
680 TEER in these wells were also significantly less compared to controls (in 100 µg/ml  
681 highly significant,  $P < 0.01$ ) (Figure 2B). Furthermore, a significant drop in TEER was  
682 observed after application of *P.gingivalis* OMVs (0.3 and 50 µg/ml) ( $P < 0.05$ ) which  
683 were highly significant after application of 0.1 and 100µg/ml ( $P < 0.01$ ) (Figure 6A).  
684 The recovery in the wells with 50 and 100µg/ml had a highly significant ( $P < 0.001$ )  
685 deficit compared to the controls (Figure 6B), indicating that these virulence factors  
686 affected the *in vitro* BBB model in a prolonged and negative fashion. However, at  
687 lower concentrations (0.1, 0.3 and 1 µg/ml) some of the TEER value reductions were  
688 temporary followed by partial or complete recovery (Figure 6B). The authors suggest  
689 this may have arisen as a result of i) an initial apoptosis event subsequently  
690 overcome by the surviving neighbouring cells expanding to repair the damaged area  
691 or ii) an initial disruption of the tight junction complexes followed by a reparatory  
692 upregulation event. These observations are important as they indicate the cells of  
693 the BBB model have an ability to recover if the endotoxin is applied at a low level.  
694 Applied to a human clinical scenario this means that after a low level, low frequency  
695 endotoxin contact with the BBB, the NVU cells appear to retain the ability to  
696 preserve the barrier's integrity. Clinically this could correlate with the adoption of an  
697 improvement in oral hygiene or if systemic risk factors for PD, such as diabetes, were  
698 eliminated or reduced.

699 The wells demonstrating less ability to recover their TEER values, could indicate that  
700 the cells in those wells were unable to survive or expand, or the LPS and OMV could  
701 have influenced the continuity of the cell layer either by causing pyroptosis [38],  
702 apoptosis or irreversible tight junction disruption [43,60]. It was recorded that there

703 were reductions in TEER readings in the wells receiving FITC *P.gingivalis* LPS  
704 conjugate in media compared to controls and that these TEER levels also did not  
705 recover as well, though none of these TEER value differences were statistically  
706 significant compared to the controls (Figure 4A and  
707 4B).

708 The appearance of FITC dextran in the basolateral compartment gave an indication  
709 of disruption to the barrier integrity after unconjugated *P.gingivalis* LPS and OMV  
710 application at various concentrations. Average Papp values were then calculated at  
711 60 min, 120 min and 240 min and were found to be  $1.04 \times 10^{-8}$  cm/s,  $8.7 \times 10^{-8}$  cm/s  
712 and  $4.8 \times 10^{-8}$  cm/s. In permeability assays for drug transportation poor permeability  
713 is indicated by Papp values of 0 -  $1.4 \times 10^{-6}$  cm/s and high permeability by values in the  
714 range of  $5 \times 10^{-5}$  -  $9 \times 10^{-5}$  cm/s. The low calculated Papp values in our study suggest  
715 that the Papp for the tracer compound FITC-dextran were low indicating the BBB  
716 model retained its overall barrier function for the first two hours, though allowing  
717 enough permeation to measure a difference between test wells (Figure 3). The most  
718 significant effect in the models TEER measurements were observed in the wells with  
719 concentrations of unconjugated LPS and OMV at 0.3  $\mu$ g/ml, 10  $\mu$ g/ml, 50  $\mu$ g/ml and  
720 100  $\mu$ g/ml and contextualised to a theoretical physiological condition, the lowest of  
721 these values, 0.3  $\mu$ g/ mL is most clinically applicable [7,59].

722 The changes in the BBB model cells after application of the FITC-*P.gingivalis* LPS in  
723 conjunction with 10  $\mu$ g/ml of *P.gingivalis* OMV showed a significant difference in the  
724 magnitude of change in the TEER values and a significant deficit in recovery of the  
725 values (highly significant in 100  $\mu$ g/ml FITC-*P.gingivalis* LPS) which, highlighted the  
726 potency of the OMVs containing gingipains pr (Figure 8).

727 The TEER measurements of an *in vitro* BBB model reflect the ionic conduction  
728 paracellularly in the cell layers, whereas the percentage appearance of a tracer  
729 compound in the BLC represents paracellular waterflow associated with increased  
730 pore size at the tight junctions [52]. Transcellular ion transport function and  
731 paracellular permeability of solute transport are differentially regulated [52], where  
732 the factors affecting perfusion of a molecule across the BBB is size, shape and  
733 lipophilicity. TEER is a valuable assessment of the *in vitro* BBB integrity as it is easy to  
734 quantify and if carried out with care, non-invasive. It is however important to be  
735 aware of the limitations of TEER measurements, where variations can occur due to  
736 factors such as medium content, temperature and the passage numbers in the cell  
737 lines at the time of measurements [52]. As the protocols in this study were  
738 performed under the same conditions using the same equipment and cell passage  
739 numbers, some of the potential variables could be excluded. As an example, the  
740 EVOM probe was calibrated in the same manner before each measurement and five  
741 readings were taken from the individual wells with each experiment, providing the  
742 authors with confidence in the longitudinal magnitude of change and TEER endpoint  
743 results

744 The biphasic TEER pattern observed in all the virulence factor application protocols  
745 (data not shown) could potentially also be explained by the exponential growth of  
746 the cells in the wells or a cell response to the applied reagents such as an  
747 upregulation in the cells, making the TEER appear to recover with time. This would  
748 suggest that any disruptions to the BBB cells which could be measurable by TEER,  
749 would have to counteract this progression in cell density and tight junction  
750 maturation or would otherwise go undetected. It is most likely that the recovery of  
751 the BBB observed in the wells, throughout our experiments, reflects an increased  
752 number of cells in the BBB as there was no other significant increases in permeability

753 recorded for the remainder of the test period when further endotoxin was applied,  
754 or the concentrations of LPS added were not high enough to induce measurable  
755 changes to the percentage appearance in the BLC (Figures 3 and 5).

756 Previous validation studies of *in vitro* BBB models like ours have shown that a TEER  
757 (read) value in the range of 120 – 130 ohms/cm<sup>2</sup> is enough for transport studies [61].  
758 When setting up the BBB model for testing transport and permeability in this project  
759 the aim was to achieve values of TEER (read) – TEER (blank) ≥ 260 ohms/cm<sup>2</sup> [61],  
760 this was achieved in all the  
761 protocols.

762 A tracer compound used in an *in-vitro* BBB model can potentially interfere with the  
763 test reagents and affect the integrity of the barrier [52]. This issue was addressed by  
764 using test wells with FITC-dextran only throughout the study. Fluorophore and dye  
765 tracer compounds are not always sensitive enough to show subtle changes in barrier  
766 model permeability [52] which is a weakness of this type of study and bias can be  
767 introduced if the sensitivity in the measuring equipment is not high enough to pick  
768 up the compound at small levels. The FITC dextran molecule used here has been  
769 shown to cross the BBB model via intercellular diffusion [62] and any increase in  
770 intercellular channels would allow greater amounts to pass into the BLC. This study  
771 demonstrated that the appearance of FITC dextran into the BLC occurred early  
772 (between 1 and 4 hours) after the initial application of unconjugated *P.gingivalis* LPS,  
773 particularly with the testing of the higher concentrations of LPS, but subsequent  
774 applications failed to demonstrate any clear correlation between the concentration  
775 of applied endotoxin and the percentage appearance measured in the BLC. This  
776 implies that the higher concentrations of LPS were able to induce an increase in  
777 paracellular flow, possibly by increasing paracellular gaps, at initial application

778 compared to controls (Figure 3). However, further increases were not demonstrated  
779 by additional applications implying a finite capacity for paracellular flow increase.  
780 These findings were supported by the Papp calculations of the FITC dextran  
781 throughout the protocols and the percentage appearance values which also  
782 remained low after application of unconjugated LPS. The levels of FITC-dextran  
783 appearance seen throughout the unconjugated LPS experiments were persistently  
784 low with the maximum appearance at 0.7% (Figure 3) which is encouraging in terms  
785 of demonstrating the quality of the barrier model [50]. In comparison the  
786 percentage appearance of FITC dextran seen in the OMV alone experiment were  
787 higher with the maximum percentage appearance being 15-fold higher than the LPS  
788 alone (Figure 7). The maximum percentage appearance of the FITC LPS conjugate in  
789 the BLC was 5% during the experiments (Figure 5) and a small increase to 8%  
790 maximum percentage appearance was observed when 10 µg/ml was added to the  
791 FITC-LPS conjugate (Figure 9). The increased percentage appearance in the OMV  
792 alone (Figure 7) could be explained by the presence of the proteolytic enzymes or  
793 gingipains within the OMVs which could also explain the increased permeability of  
794 the FITC *P.gingivalis* LPS in the presence of 10 µg/ml of OMV (Figure 9). The enzymes  
795 could create greater gaps between the barriers cell layers allowing greater perfusion  
796 of the molecules to the BLC. The differences in percentage appearance between  
797 the FITC *P.gingivalis* LPS and the FITC dextran molecules (Figures 3 and 5), where the  
798 percentage detected in the BLC of FITC *P.gingivalis* LPS was approximately 5 fold  
799 larger than FITC dextran appearance after unconjugated LPS, can be explained as a  
800 potential difference in the virulence between the two compounds (conjugated and  
801 unconjugated LPS) inflicting different effects on the pore sizes within the barrier, or  
802 variances in the size, shape and/or lipophilicity between FITC dextran and FITC LPS  
803 molecules could attribute to this observation. The *P.gingivalis* LPS could also affect



804 the cells of the BBB model differently at receptor level after being conjugated , even  
805 though the LPS product used for both reagents originated from the same source.

806 The immune response of the *P.gingivalis* LPS, *P.gingivalis* LPS FITC conjugate and  
807 *P.gingivalis* OMV utilised in the experiments was examined by an IL-6 ELISA after  
808 application for 4 hours to HBPC. IL6 is a proinflammatory cytokine and the induction  
809 of this cytokine would give an indication of the biological activity of the virulence  
810 factors utilised in this study, as the presence of LPS would induce TNF- $\alpha$  pathways in  
811 the HBPC to release IL6 [63]. The response and induction of IL-6 from all reagents  
812 measured in the cell media, were of a similar quantity and levels were increased  
813 compared to controls (media only)(data not shown).

814 The unconjugated *P.gingivalis* LPS used in this study was the standard preparation  
815 (defined by preparation by supplier) which has been noted to induce a stronger  
816 inflammatory response than the pure version (both supplied by Invivogen) possibly  
817 as a result of impurities of lipoproteins in the standard preparation, activating TLR2  
818 as well as TLR4 [64]. Furthermore, the standard *P.gingivalis* LPS has also been found  
819 to show a stronger inflammatory response in human periodontal stem cells after 24  
820 hours than the pure version (64). In our BBB protocols we saw an increased response  
821 at 24 hours with both *P.gingivalis* LPS and OMVs which indicates that the induced  
822 response could be more complex than a simple apoptosis of the cells and involve  
823 inflammatory pathways affecting the integrity of the barrier. The OMVs applied in  
824 this study were extracted from a culture of the laboratory strain *P.gingivalis* FDC 381  
825 which is classed as a less virulent *P.gingivalis* strain but has a high ability to be  
826 internalized in human cells [65]. This non-capsular strain has been shown to be a  
827 strong immune stimulant, (even activating TLR2) a property attributed to an intact  
828 fimB allele but with a less gingipain activity [66]. It is possible that the difference in  
829 appearance of the *P.gingivalis* LPS FITC conjugate on the CNS side of the model with

830 and without the presence of the OMVs would have been more significant if a less  
831 virulent *P.gingivalis* LPS product had been used such as the purified product  
832 mentioned previously.

833 The *in vitro* BBB model has limitations such as the delicate nature of working with  
834 primary-derived cell lines and the measurements derived from this study do not  
835 divulge much information about a cellular level activity. There is an increased  
836 consensus that to gain more accurate knowledge of AD, microbial pathology human  
837 models need to be developed, as pathological and inflammatory pathways in  
838 rodents significantly differ from humans [6, 31] especially in relation to molecules  
839 such as LPS [38]. The expression in the author's human BBB model cells is closer to  
840 the *in vivo* state than a murine model and there is potential in our model to gain  
841 further cellular level information. The role of microglial cells in neurodegeneration is  
842 undisputed and expansion of this model to include human microglial cells could  
843 broaden the applications for this type of protocol. In addition, also BBB organoids  
844 could potentially be applied to this type of study [67].

845 There is evidence to suggest that *P.gingivalis* may not need to enter the brain to  
846 cause neuroinflammation [38]. Even healthy humans have been shown to have low  
847 levels of LPS in their blood [68], but this is found to be elevated in AD and PD  
848 patients [69,70,71]. AD patients have been found to have 2-3 times as much LPS in  
849 the brains as healthy individuals [72]. LPS is released from the bacteria either when  
850 it is degraded or when outer membrane vesicles are released [38] and the GI  
851 microbiome has been shown to be the main contributor to systemic presence. LPS  
852 has been suggested as an intermediary between bacteria and the CNS at low levels  
853 (physiological) conditions [73] in rodents, and a lipo-protein transport mechanism to  
854 the CNS has been suggested, but it is not yet known exactly how LPS enters the brain

855 in humans. It is possible that transport mechanisms are responsible for the  
856 appearance of the LPS on the BLC (CNS) side of the model used in this study and this  
857 topic warrants further investigation, OMVs are known to have the ability to be  
858 internalised by human cells which is another avenue to explore.

859 This study however has demonstrated that the integrity of a BBB model is reduced  
860 by the presence of *P.gingivalis* virulence factors seen by a measurable reduction in  
861 TEER levels and making the barrier more permeable and the subsequent increased  
862 appearance of LPS in the BLC (CNS side of BBB).

863 Bacterial LPS has been found to change the permeability of the BBB at high doses  
864 [74] as seen in sepsis causing significant CNS disability. *P.gingivalis* LPS has the  
865 potential to cause neuroinflammation via the blood directly acting at the BBB, by  
866 inducing pro-inflammatory cytokines, initiating pro inflammatory pathways in the  
867 tissues of the neuro vascular unit and activating microglial cells without entering the  
868 brain [38]. In addition, this study has indicated that *P.gingivalis* LPS also has the  
869 potential to cross the BBB as seen in the FITC *P.gingivalis* LPS experiments,  
870 potentially explaining how systemic circulating LPS could induce neuroinflammation.

871 The subsequent immunological response to LPS is well documented (for a review see  
872 44) and the toxicity of an endotoxin is determined by how the host reacts to it [75].

873 Both immunological activation and tolerance [76,77] can explain how chronic  
874 exposure to even medium and low levels of *P.gingivalis* LPS could lead to  
875 neurodegeneration by induction of pro-inflammatory pathways and activation of  
876 microglia and it is plausible that a low concentration of *P.gingivalis* virulence factors  
877 can induce damage to the NVU cells [78,79]. Here we have shown, in a BBB model,  
878 that whole bacteria do not need to be present as *P.gingivalis* LPS and OMVs have the  
879 armoury to induce alteration of the barrier integrity providing access to the CNS  
880 tissues. A question remains about how much damage, over what period of time is

881 required, before the balance is tipped towards a path where the BBB cells cannot  
882 recover?

883 The aim of applying *P.gingivalis* LPS and OMVs to a HBMEC monolayer was to  
884 investigate whether the changes observed in the BBB model protocols could be seen  
885 at a cellular level and to determine how these changes occurred. The negative  
886 control cells (no virulence factors applied) showed the expected position of the ZO-1  
887 protein at the cell-cell junctions [80] with the signal of the ZO-1 protein appearing  
888 well organised (Figure 10B and 10C). The HBMEC monolayer with application of  
889 *P.gingivalis* LPS showed no noticeable effect on the ZO-1 signal (Figure 10 D-F) (only  
890 0.3 µg/ml shown) and similar observations were made in the wells with 0.1 µg/ml  
891 *P.gingivalis* OMV application (Figure 10 G-I) compared to the untreated controls  
892 (media only). The wells with application of 0.3 µg/ml *P.gingivalis* OMVs showed a  
893 more diffused signal from the ZO-1 proteins compared to untreated controls, which  
894 could appear as a reduction in the signal (Figure 10 J-L). All the test wells and  
895 controls were imaged using the same exposure times and all post exposure  
896 modifications were carried out to the same level with the Zen software. Though a  
897 change in the Cy5 signal after the application of 0.3 µg/ml *P.gingivalis* OMVs were  
898 seen in all 3 repeat experiments compared to untreated controls, it was not clear if  
899 the change was a displacement of the ZO-1 protein or reduced numbers as the  
900 experiment here did not quantify the protein. ZO-1 is a tight junction adaptor  
901 protein connecting the actin skeleton to tight junctions such as claudin and the  
902 binding of Zo-1 to actin is essential for regulation of permeability in epithelial cells  
903 [81]. Tornavaca et al. (2015)[82] showed that in primary endothelial cells ZO-1 is a  
904 central regulator of tight junctions depending on the strictly endothelial specific  
905 adhesion molecule vascular endothelial (VE) -cadherin. These endothelial junctions  
906 were found to influence the spatial actomyosin organization, cell–cell tension and

907 migration across the endothelium, but also angiogenesis and barrier formation. This  
908 study used human dermal microvascular endothelial cells (HDMEC-c) and not  
909 HBMECs, but this places ZO-1 central to the development, integrity and maintenance  
910 of the BBB and if *P.gingivalis* OMVs are able to disrupt the functionality of ZO-1 this  
911 could have devastating consequences to the integrity of the blood brain interface.  
912 ZO-1 is a large phosphoprotein and post-translational alterations such as  
913 phosphorylation would lead to ZO-1 dissociation from the tight junction complex  
914 [83], which could potentially be how *P.gingivalis* virulence factors affect this protein  
915 and explain the TEER and diffusion changes observed in our study, where notably the  
916 application of *P.gingivalis* OMVs had the greatest effect on both measurements.

917 Multiple studies have investigated the effect of *P.gingivalis* LPS and OMVs on cells,  
918 both human and animal, but not on cells of the human BBB. It was clear from our  
919 study that the *P.gingivalis* LPS both unconjugated and FITC conjugated and OMVs did  
920 affect the cells of this *in vitro* BBB model and caused barrier integrity changes. There  
921 is potential to investigate more nuanced changes in the cells by using the protocol  
922 described here and applying further protocols which could also potentially reveal  
923 changes at the lower concentration of LPS level which the TEER and percent  
924 appearance methods did not have the sensitivity to reveal.

## 925 CONCLUSION

926 The two virulence factors of *P.gingivalis* (LPS and OMVs) were seen to induce  
927 changes in the human *in vitro* BBB model cells. Unconjugated *P.gingivalis* LPS, FITC  
928 conjugated *P.gingivalis* LPS with 10 µg/ml of OMV and OMVs alone had a significant  
929 effect on the integrity of the *in vitro* BBB model which were measurable by TEER  
930 showing a significantly greater magnitude of change after application and a  
931 significant deficit in recovery of the models TEER values. These changes were also

932 observed after application of virulence factors at a physiological relevant level (0.3  
933  $\mu\text{g/ml}$ ). The application of *P.gingivalis* OMVs resulted in the most significant  
934 magnitude of change in the TEER values of the barrier and the most significant  
935 deficit of recovery. These experiments also confirmed that endotoxin from  
936 *P.gingivalis* conjugated with FITC was able to cross the barrier model and that the  
937 percentage of LPS conjugate appearing on the CNS side of the model were increased  
938 by the presence of *P.gingivalis* OMVs. The ZO-1 proteins in a HBMEC monolayer  
939 model showed disruption after contact with *P.gingivalis* OMVs compared to  
940 controls.

941 Further investigations at cellular level are warranted to contribute to the knowledge  
942 pool of how endotoxin from periodontal disease could have an influence on  
943 neuroinflammatory states and potentially contribute to or exacerbate  
944 neurodegeneration. If these observations are applied to the human BBB, then  
945 infection with *P.gingivalis* and their inflammagens LPS and OMVs could cause  
946 damage to an otherwise healthy and non-predisposed individual. It is tempting to  
947 attribute the link between sporadic Alzheimer's Disease and periodontal disease to  
948 the effect of this multi-talented pathogen, when the chronicity of the inflammatory  
949 state seen in established periodontal disease could be the main culprit. This  
950 highlights not only the need for good oral hygiene, but also the importance of  
951 diagnosis and optimal management of dental patients presenting with unstable  
952 periodontal disease. Until there is a therapeutic remedy which can protect the BBB  
953 from chronic inflammation, prevention remains the key.

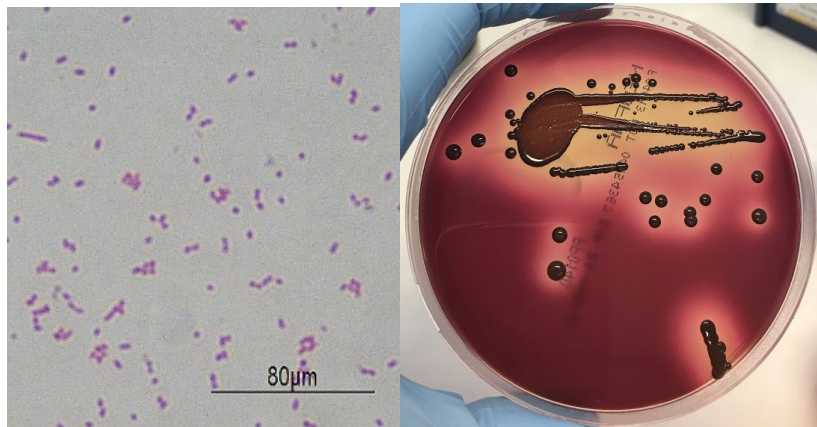
954 ACKNOWLEDGEMENTSAP acknowledges funding from the Faculty of Dental Surgery,  
955 Royal College of Surgeons England pump priming grant and the kind donation from  
956 The Norah and Fred Roberts Memorial Trust.

957 CONFLICT OF INTEREST

958 The authors declare no conflict of interest.

959

960 Supplementary information:



961

962 *P.gingivalis* FDC 381 Gram stain and on FAA Neomycin (E&O, UK) shows  
963 coccobacillus at x100 and Black stain colonies of the strain with haemolytic halos on  
964 NEOFAA agar.

965

966 References

- 967 1. Alonso R, Pisa D, Marina AI, Morato E, Rábano A, Carrasco L. Fungal infection in patients with  
968 Alzheimer's disease. J Alzheimers Dis. 2014;41(1):301-11. doi: 10.3233/JAD-132681. PMID:  
969 24614898.
- 970 2. Miklossy J. Bacterial Amyloid and DNA are Important Constituents of Senile Plaques: Further  
971 Evidence of the Spirochetal and Biofilm Nature of Senile Plaques. J Alzheimers Dis. 2016 Jun  
972 13;53(4):1459-73. doi: 10.3233/JAD-160451. PMID: 27314530; PMCID: PMC4981904.
- 973 3. Itzhaki RF, Lin WR, Shang D, Wilcock GK, Faragher B, Jamieson GA. Herpes simplex virus type  
974 1 in brain and risk of Alzheimer's disease. Lancet. 1997 Jan 25;349(9047):241-4. doi: 10.1016/S0140-  
975 6736(96)10149-5. PMID: 9014911.
- 976 4. Pritchard AB, Crean S, Olsen I, Singhrao SK. Periodontitis, Microbiomes and their Role in  
977 Alzheimer's Disease. Front Aging Neurosci. 2017 Oct 24;9:336. doi: 10.3389/fnagi.2017.00336. PMID:  
978 29114218; PMCID: PMC5660720.
- 979 5. Braak H, Braak E. Morphologie des Morbus Alzheimer [Morphology of Alzheimer disease].  
980 Fortschr Med. 1990 Nov 20;108(33):621-4. German. Erratum in: Fortschr Med 1991 Mar  
981 20;109(8):186. PMID: 2289729.

- 982 6. Fulop T, Tripathi S, Rodrigues S, Desroches M, Bunt T, Eiser A, Bernier F, Beauregard PB,  
983 Barron AE, Khalil A, Plotka A, Hirokawa K, Larbi A, Bocti C, Laurent B, Frost EH, Witkowski JM.  
984 Targeting Impaired Antimicrobial Immunity in the Brain for the Treatment of Alzheimer's Disease.  
985 *Neuropsychiatr Dis Treat.* 2021 May 4;17:1311-1339. doi: 10.2147/NDT.S264910. PMID: 33976546;  
986 PMCID: PMC8106529.
- 987 7. Guo, T., Zhang, D., Zeng, Y. et al. Molecular and cellular mechanisms underlying the  
988 pathogenesis of Alzheimer's disease. *Mol Neurodegeneration* 15, 40 (2020).  
989 <https://doi.org/10.1186/s13024-020-00391-7>
- 990 8. Sevenich Lisa, Brain-Resident Microglia and Blood-Borne Macrophages Orchestrate Central  
991 Nervous System Inflammation in Neurodegenerative Disorders and Brain Cancer, *Frontiers in*  
992 *Immunology*, Vol. 9, 2018, p 697, <https://www.frontiersin.org/article/10.3389/fimmu.2018.00697>,  
993 DOI=10.3389/fimmu.2018.00697, ISSN=1664-3224
- 994 9. Soccia SJ, Kirby JE, Washicosky KJ, et al. The Alzheimer's disease-associated amyloid beta-  
995 protein is an antimicrobial peptide. *PLoS One.* 2010;5(3):e9505. doi:10.1371/journal.pone.0009505
- 996 10. Kumar DK, Choi SH, Washicosky KJ, et al. Amyloid- $\beta$  peptide protects against microbial  
997 infection in mouse and worm models of Alzheimer's disease. *Sci Transl Med.* 2016;8(340):340ra72.  
998 doi:10.1126/scitranslmed.aaf1059
- 999 11. Hajishengallis G, Darveau RP, Curtis MA. The keystone-pathogen hypothesis. *Nat Rev*  
1000 *Microbiol.* 2012;10(10):717–725.
- 1001 12. Hajishengallis G, Lamont RJ. Beyond the red complex and into more complexity: the  
1002 polymicrobial synergy and dysbiosis (PSD) model of periodontal disease etiology. *Mol Oral Microbiol.*  
1003 2012;27(6):409–419.
- 1004 13. Olsen, I., Kell, D. B., & Pretorius, E. (2020). Is *Porphyromonas gingivalis* involved in  
1005 Parkinson's disease?. *European journal of clinical microbiology & infectious diseases* : official  
1006 publication of the European Society of Clinical Microbiology, 39(11), 2013–2018.  
1007 <https://doi.org/10.1007/s10096-020-03944-2>
- 1008 14. Holmstrup P, Damgaard C, Olsen I, Klinge B, Flyvbjerg A, Nielsen CH, Hansen PR. Comorbidity  
1009 of periodontal disease: two sides of the same coin? An introduction for the clinician. *J Oral*  
1010 *Microbiol.* 2017;9(1):1332710.
- 1011 15. Kozak, M., Dabrowska-Zamojcin, E., Mazurek-Mochol, M., & Pawlik, A. (2020). Cytokines and  
1012 Their Genetic Polymorphisms Related to Periodontal Disease. *Journal of clinical medicine*, 9(12),  
1013 4045. <https://doi.org/10.3390/jcm9124045>
- 1014 16. Forner L, Larsen T, Kilian M, Holmstrup P. Incidence of bacteremia after chewing, tooth  
1015 brushing and scaling in individuals with periodontal inflammation. *J Clin Periodontol.* 2006  
1016 Jun;33(6):401-7. doi: 10.1111/j.1600-051X.2006.00924.x. PMID: 16677328.
- 1017 17. Dominy SS, Lynch C, Ermini F, Benedyk M, Marczyk A, Konradi A, Nguyen M, Haditsch U,  
1018 Raha D, Griffin C, Holsinger LJ, Arastu-Kapur S, Kaba S, Lee A, Ryder MI, Potempa B, Mydel P,  
1019 Hellvard A, Adamowicz K, Hasturk H, Walker GD, Reynolds EC, Faull RLM, Curtis MA, Dragunow M,  
1020 Potempa J. *Porphyromonas gingivalis* in Alzheimer's disease brains: Evidence for disease causation  
1021 and treatment with small-molecule inhibitors. *Sci Adv.* 2019 Jan 23;5(1):eaau3333. doi:  
1022 10.1126/sciadv.aau3333. PMID: 30746447; PMCID: PMC6357742.



- 1023 18. Poole S, Singhrao SK, Kesavalu L, Curtis MA, Crean S (2013) Determining the presence of  
1024 periodontopathic virulence factors in short-term postmortem Alzheimer's disease brain tissue. *J*  
1025 *Alzheimers Dis* 36, 665–677.
- 1026 19. Poole S, Singhrao SK, Chukkapalli S, Rivera M, Velsko I, Kesavalu L, Crean SJ. Active invasion  
1027 of *Porphyromonas gingivalis* and infection-induced complement activation in ApoE<sup>-/-</sup> mice brains. *J*  
1028 *Alzheimers Dis*. 2015;43(1):67–80.
- 1029 20. Ilievski V, Zuchowska PK, Green SJ, Toth PT, Ragozzino ME, Le K, Aljewari HW, O'Brien-  
1030 Simpson NM, Reynolds EC, Watanabe K (2018) Chronic oral application of a periodontal pathogen  
1031 results in brain inflammation, neurodegeneration and amyloid beta production in wild type mice.  
1032 *PLoS One* 13, e0204941.
- 1033 21 Dorn BR, Burks JN, Seifert KN, Progulske-Fox A. Invasion of endothelial and epithelial cells by  
1034 strains of *Porphyromonas gingivalis*. *FEMS Microbiol Lett*. 2000;187:139–44.
- 1035 22 Yoshino T, Laine ML, Van Winkelhoff AJ, Dahlén G, Genotype variation and capsular  
1036 serotypes of *Porphyromonas gingivalis* from chronic periodontitis and periodontal abscesses, *FEMS*  
1037 *Microbiology Letters*, Volume 270, Issue 1, May 2007, Pages 75–81, [https://doi.org/10.1111/j.1574-](https://doi.org/10.1111/j.1574-6968.2007.00651.x)  
1038 [6968.2007.00651.x](https://doi.org/10.1111/j.1574-6968.2007.00651.x)
- 1039 23 Ha JY, Choi SY, Lee JH, Hong SH, Lee HJ. Delivery of Periodontopathogenic Extracellular  
1040 Vesicles to Brain Monocytes and Microglial IL-6 Promotion by RNA Cargo. *Front Mol Biosci*. 2020 Nov  
1041 24;7:596366. doi: 10.3389/fmolb.2020.596366. PMID: 33330627; PMCID: PMC7732644.
- 1042 24 Veith PD, Chen YY, Gorasia DG, Chen D, Glew MD, O'Brien-Simpson NM, et al.  
1043 *Porphyromonas gingivalis* outer membrane vesicles exclusively contain outer membrane and  
1044 periplasmic proteins and carry a cargo enriched with virulence factors. *J Proteome Res*.  
1045 2014;13:2420–32. doi: 10.1021/pr401227e.
- 1046 25 Abe N, Kadowaki T, Okamoto K, Nakayama K, Ohishi M, Yamamoto K. Biochemical and  
1047 functional properties of lysine-specific cysteine proteinase (Lys-gingipain) as a virulence factor of  
1048 *Porphyromonas gingivalis* in periodontal disease. *J Biochem*. 1998 Feb;123(2):305-12. doi:  
1049 10.1093/oxfordjournals.jbchem.a021937. PMID: 9538207.
- 1050 26 Olsen, I., & Amano, A. (2015). Outer membrane vesicles - offensive weapons or good  
1051 Samaritans?. *Journal of oral microbiology*, 7, 27468. <https://doi.org/10.3402/jom.v7.27468>
- 1052 27 Furuta N, Takeuchi H, Amano A. Entry of *Porphyromonas gingivalis* outer membrane vesicles  
1053 into epithelial cells causes cellular functional impairment. *Infect Immun*. 2009;77:4761–70. doi:  
1054 10.1128/IAI.00841-09.
- 1055 28 Hajishengallis G. (2011). Immune evasion strategies of *Porphyromonas gingivalis*. *Journal of*  
1056 *oral biosciences*, 53(3), 233–240. <https://doi.org/10.2330/joralbiosci.53.233>
- 1057 29 Meghil, M. M., Tawfik, O. K., Elashiry, M., Rajendran, M., Arce, R. M., Fulton, D. J.,  
1058 Schoenlein, P. V., & Cutler, C. W. (2019). Disruption of Immune Homeostasis in Human Dendritic  
1059 Cells via Regulation of Autophagy and Apoptosis by *Porphyromonas gingivalis*. *Frontiers in*  
1060 *immunology*, 10, 2286. <https://doi.org/10.3389/fimmu.2019.02286>
- 1061 30 Deatherage BL, Cookson BT. Membrane vesicle release in bacteria, eukaryotes, and archaea:  
1062 a conserved yet underappreciated aspect of microbial life. *Infect Immun*. 2012;80:1948–57.

1063 31 Nativel, B., Couret, D., Giraud, P. et al. Porphyromonas gingivalis lipopolysaccharides act  
1064 exclusively through TLR4 with a resilience between mouse and human. *Sci Rep* 7, 15789 (2017).  
1065 <https://doi.org/10.1038/s41598-017-16190-y>

1066 32 Muoio V, Persson PB, Sendeski MM. The neurovascular unit - concept review. *Acta Physiol*  
1067 (Oxf). 2014 Apr;210(4):790-8. doi: 10.1111/apha.12250. PMID: 24629161.

1068 33 Cipolla MJ. *The Cerebral Circulation*. San Rafael (CA): Morgan & Claypool Life Sciences; 2009.  
1069 Chapter 2, Anatomy and Ultrastructure. Available from:  
1070 <https://www.ncbi.nlm.nih.gov/books/NBK53086>.

1071 34 Sweeney MD, Sagare AP, Zlokovic BV. Blood-brain barrier breakdown in Alzheimer disease  
1072 and other neurodegenerative disorders. *Nat Rev Neurol*. 2018 Mar;14(3):133-150. doi:  
1073 10.1038/nrneurol.2017.188. Epub 2018 Jan 29. PMID: 29377008; PMCID: PMC5829048.

1074 35 Anette Wolff, Maria Antfolk, Birger Brodin, Maria Tenje, *In Vitro Blood–Brain Barrier*  
1075 *Models—An Overview of Established Models and New Microfluidic Approaches*, *Journal of*  
1076 *Pharmaceutical Sciences*, Volume 104, Issue 9, 2015, Pages 2727-2746, ISSN 0022-3549,  
1077 <https://doi.org/10.1002/jps.24329>.

1078 36 Verheggen, I.C.M., de Jong, J.J.A., van Boxtel, M.P.J. et al. Increase in blood–brain barrier  
1079 leakage in healthy, older adults. *GeroScience* 42, 1183–1193 (2020).  
1080 <https://doi.org/10.1007/s11357-020-00211-2>

1081 37 Lochhead Jeffrey J., Yang Junzhi, Ronaldson Patrick T., Davis Thomas P.,  
1082 Structure, Function, and Regulation of the Blood-Brain Barrier Tight Junction in Central Nervous  
1083 System Disorders, *Frontiers in Physiology*, 11, 2020,914,  
1084 URL=<https://www.frontiersin.org/article/10.3389/fphys.2020.00914> DOI=10.3389/fphys.2020.00914  
1085

1086 38 Brown GC. The endotoxin hypothesis of neurodegeneration. *J Neuroinflammation*. 2019 Sep  
1087 13;16(1):180. doi: 10.1186/s12974-019-1564-7. PMID: 31519175; PMCID: PMC6744684.  
1088

1089 39 Methia N, André P, Hafezi-Moghadam A, Economopoulos M, Thomas KL, Wagner DD. ApoE  
1090 deficiency compromises the blood brain barrier especially after injury. *Mol Med*. 2001  
1091 Dec;7(12):810-5. PMID: 11844869; PMCID: PMC1950012.

1092 40 Montagne, A., Nation, D.A., Sagare, A.P. et al. APOE4 leads to blood–brain barrier  
1093 dysfunction predicting cognitive decline. *Nature* 581, 71–76 (2020). <https://doi.org/10.1038/s41586-020-2247-3>  
1094

1095 41 Dando SJ, Mackay-Sim A, Norton R, et al. Pathogens penetrating the central nervous system:  
1096 infection pathways and the cellular and molecular mechanisms of invasion. *Clin Microbiol Rev*.  
1097 2014;27(4):691–726. doi:10.1128/CMR.00118-13

1098 42 Coureuil M, Lécuyer H, Bourdoulous S, Nassif X. A journey into the brain: insight into how  
1099 bacterial pathogens cross blood-brain barriers. *Nat Rev Microbiol*. 2017 Mar;15(3):149-159. doi:  
1100 10.1038/nrmicro.2016.178. Epub 2017 Jan 16. PMID: 28090076.

- 1101 43 Takeuchi, H., Sasaki, N., Yamaga, S., Kuboniwa, M., Matsusaki, M., & Amano, A. (2019).  
1102 Porphyromonas gingivalis induces penetration of lipopolysaccharide and peptidoglycan through the  
1103 gingival epithelium via degradation of junctional adhesion molecule 1. PLoS pathogens, 15(11),  
1104 e1008124. <https://doi.org/10.1371/journal.ppat.1008124>
- 1105 44 Sheets, S. M., Potempa, J., Travis, J., Casiano, C. A., & Fletcher, H. M. (2005). Gingipains from  
1106 Porphyromonas gingivalis W83 induce cell adhesion molecule cleavage and apoptosis in endothelial  
1107 cells. Infection and immunity, 73(3), 1543–1552. <https://doi.org/10.1128/IAI.73.3.1543-1552.2005>
- 1108 45 Yuhan He, Noriko Shiotsu, Yoko Uchida-Fukuhara, Jiajie Guo, Yao Weng, Mika Ikegame, Ziyi  
1109 Wang, Kisho Ono, Hiroshi Kamioka, Yasuhiro Torii, Akira Sasaki, Kaya Yoshida, Hirohiko Okamura,  
1110 Outer membrane vesicles derived from Porphyromonas gingivalis induced cell death with disruption  
1111 of tight junctions in human lung epithelial cells, Archives of Oral Biology, Volume 118, 2020, 104841,  
1112 ISSN 0003-9969, <https://doi.org/10.1016/j.archoralbio.2020.104841>.
- 1113 46 Solleiro-Villavicencio H, Rivas-Arancibia S, Effect of Chronic Oxidative Stress on  
1114 Neuroinflammatory Response Mediated by CD4+T Cells in Neurodegenerative Diseases, Frontiers in  
1115 Cellular Neuroscience, 12, 2018,114  
1116 URL=<https://www.frontiersin.org/article/10.3389/fncel.2018.00114>  
1117 DOI=10.3389/fncel.2018.00114
- 1118 47 Banks, W.A., Gray, A.M., Erickson, M.A. et al. Lipopolysaccharide-induced blood-brain barrier  
1119 disruption: roles of cyclooxygenase, oxidative stress, neuroinflammation, and elements of the  
1120 neurovascular unit. J Neuroinflammation 12, 223 (2015). [https://doi.org/10.1186/s12974-015-0434-](https://doi.org/10.1186/s12974-015-0434-1)  
1121 1
- 1122 48 Wang, X., Xue, G.-X., Liu, W.-C., Shu, H., Wang, M., Sun, Y., Liu, X., Sun, Y.E., Liu, C.-F., Liu, J.,  
1123 Liu, W. and Jin, X. (2017), Melatonin alleviates lipopolysaccharide-compromised integrity of blood–  
1124 brain barrier through activating AMP-activated protein kinase in old mice. Aging Cell, 16: 414-421.  
1125 <https://doi.org/10.1111/accel.12572>
- 1126 49 Pflanzner T, Kuhlmann CR, Pietrzik CU. Blood-brain-barrier models for the investigation of  
1127 transporter- and receptor-mediated amyloid- $\beta$  clearance in Alzheimer's disease. Curr Alzheimer Res.  
1128 2010 Nov;7(7):578-90. doi: 10.2174/156720510793499066. PMID: 20704558.  
1129
- 1130 50 Kumar, S., Shaw, L., Lawrence, C., Lea, R. and Alder, J. (2014) 'P50 \* Developing a  
1131 Physiologically Relevant Blood Brain Barrier Model for the Study of Drug Disposition  
1132 in Glioma', Neuro-Oncology, 16(suppl 6), p. vi8-vi8. doi: 10.1093/neuonc/nou249.38  
1133
- 1134 51 Hughes, P., Marshall, D., Reid, Y., Parkes, H. & Gelber, C. (2007). The costs of using  
1135 unauthenticated, over-passaged cell lines: how much more data do we need? Biotechniques, 43,  
1136 575, 577-8, 581-2
- 1137 52 Srinivasan, B., Kolli, A. R., Esch, M. B., Abaci, H. E., Shuler, M. L., & Hickman, J. J. (2015). TEER  
1138 measurement techniques for in vitro barrier model systems. Journal of laboratory automation, 20(2),  
1139 107–126. <https://doi.org/10.1177/2211068214561025>

- 1140 53 Zwain, Tamara Akeel abdulmunim, Alder, Jane Elizabeth , Sabagh, Bassem, Shaw, Andrew,  
1141 Burrow, Andrea Julie and Singh, Kamalinder (2021) Tailoring functional nanostructured lipid carriers  
1142 for glioblastoma treatment with enhanced permeability through in-vitro 3D BBB/BBTB models.  
1143 Materials Science and Engineering: C, 121 (111774). ISSN 0928-4931
- 1144 54 Seyama M, Yoshida K, Yoshida K, Fujiwara N, Ono K, Eguchi T, Kawai H, Guo J, Weng Y, Haoze  
1145 Y, Uchibe K, Ikegame M, Sasaki A, Nagatsuka H, Okamoto K, Okamura H, Ozaki K. Outer membrane  
1146 vesicles of *Porphyromonas gingivalis* attenuate insulin sensitivity by delivering gingipains to the liver.  
1147 Biochim Biophys Acta Mol Basis Dis. 2020 Jun 1;1866(6):165731. doi: 10.1016/j.bbadis.2020.165731.  
1148 Epub 2020 Feb 20. PMID: 32088316.
- 1149 55 Danaei M, Dehghankhold M, Ataei S, Hasanzadeh Davarani F, Javanmard R, Dokhani A,  
1150 Khorasani S, Mozafari MR. Impact of Particle Size and Polydispersity Index on the Clinical  
1151 Applications of Lipidic Nanocarrier Systems. *Pharmaceutics*. 2018 May 18;10(2):57. doi:  
1152 10.3390/pharmaceutics10020057. PMID: 29783687; PMCID: PMC6027495.
- 1153 56 Helms HC, Abbott NJ, Burek M, Cecchelli R, Couraud PO, Deli MA, Förster C, Galla HJ,  
1154 Romero IA, Shusta EV, Stebbins MJ, Vandenhoute E, Weksler B, Brodin B. In vitro models of the  
1155 blood-brain barrier: An overview of commonly used brain endothelial cell culture models and  
1156 guidelines for their use. *J Cereb Blood Flow Metab*. 2016 May;36(5):862-90. doi:  
1157 10.1177/0271678X16630991. Epub 2016 Feb 11. PMID: 26868179; PMCID: PMC4853841.
- 1158 57 Іарош ОА. Математическіі анализ проницаемости гематоэнцефалического барьера при  
1159 бактериальной менингоэнцефалите [Mathematical analysis of permeability of the blood-brain barrier  
1160 in bacterial meningoencephalitis]. *Zh Nevropatol Psikhiatr Im S S Korsakova*. 1992;92(2):33-6.  
1161 Russian. PMID: 1326169.
- 1162 58. Kanoh Y, Ohara T, Akahoshi T. Acute inflammatory biomarkers in cerebrospinal fluid as  
1163 indicators of blood cerebrospinal fluid barrier damage in Japanese subjects with infectious  
1164 meningitis. *Clin Lab*. 2011;57(1-2):37-46. PMID: 21391463.
- 1165 59 Blufstein, A, Behm, C, Nguyen, PQ, Rausch-Fan, X, Andrukhov, O. Human periodontal  
1166 ligament cells exhibit no endotoxin tolerance upon stimulation with *Porphyromonas gingivalis*  
1167 lipopolysaccharide. *J Periodont Res*. 2018; 53: 589– 597. <https://doi.org/10.1111/jre.12549>  
1168
- 1169 60 Hirasawa, M., & Kurita-Ochiai, T. (2018). *Porphyromonas gingivalis* Induces Apoptosis and  
1170 Autophagy via ER Stress in Human Umbilical Vein Endothelial Cells. *Mediators of inflammation*, 2018,  
1171 1967506. <https://doi.org/10.1155/2018/1967506>
- 1172 61 Wilhelm I, Fazakas C and Krizbai I A, In vitro models of the blood-brain barrier, *Acta*  
1173 *Neurobiol Exp* 2011, 71: 113–128
- 1174 62 Hoffmann, A., Bredno, J., Wendland, M., Derugin, N., Ohara, P., & Wintermark, M. (2011).  
1175 High and Low Molecular Weight Fluorescein Isothiocyanate (FITC)-Dextrans to Assess Blood-Brain  
1176 Barrier Disruption: Technical Considerations. *Translational stroke research*, 2(1), 106–111.  
1177 <https://doi.org/10.1007/s12975-010-0049-x>
- 1178 63 Fabry Z, Fitzsimmons KM, Herlein JA, Moninger TO, Dobbs MB, Hart MN. Production of the  
1179 cytokines interleukin 1 and 6 by murine brain microvessel endothelium and smooth muscle  
1180 pericytes. *J Neuroimmunol*. 1993 Aug;47(1):23-34. doi: 10.1016/0165-5728(93)90281-3. PMID:  
1181 8376546.

- 1182 64 Behm C, Blufstein A, Abhari SY, Koch C, Gahn J, Schäffer C, Moritz A, Rausch-Fan X,  
 1183 Andrukhov O. Response of Human Mesenchymal Stromal Cells from Periodontal Tissue to LPS  
 1184 Depends on the Purity but Not on the LPS Source. *Mediators Inflamm.* 2020 Jul 2;2020:8704896. doi:  
 1185 10.1155/2020/8704896. PMID: 32714091; PMCID: PMC7352132.
- 1186 65 Olsen, I., & Progulske-Fox, A. (2015). Invasion of Porphyromonas gingivalis strains into  
 1187 vascular cells and tissue. *Journal of oral microbiology*, 7, 28788.  
 1188 <https://doi.org/10.3402/jom.v7.28788>
- 1189 66 Coats, S. R., Kantrong, N., To, T. T., Jain, S., Genco, C. A., McLean, J. S., & Darveau, R. P.  
 1190 (2019). The Distinct Immune-Stimulatory Capacities of Porphyromonas gingivalis Strains 381 and  
 1191 ATCC 33277 Are Determined by the fimB Allele and Gingipain Activity. *Infection and immunity*,  
 1192 87(12), e00319-19. <https://doi.org/10.1128/IAI.00319-19>
- 1193 67 Bergmann, S., Lawler, S. E., Qu, Y., Fadzen, C. M., Wolfe, J. M., Regan, M. S., Pentelute, B. L.,  
 1194 Agar, N., & Cho, C. F. (2018). Blood-brain-barrier organoids for investigating the permeability of CNS  
 1195 therapeutics. *Nature protocols*, 13(12), 2827–2843. <https://doi.org/10.1038/s41596-018-0066-x>
- 1196 68 Nádházi Z, Takáts A, Offenmüller K, Bertók L. Plasma endotoxin level of healthy donors. *Acta*  
 1197 *Microbiol Immunol Hung.* 2002;49:151–157. doi: 10.1556/AMicr.49.2002.1.15.
- 1198 69 Kalash D, Vovk A, Huang H, Aukhil I, Wallet SM, Shaddox LM. Influence of periodontal  
 1199 therapy on systemic lipopolysaccharides in children with localized aggressive periodontitis. *Pediatr*  
 1200 *Dent.* 2015;37:35–40.
- 1201 70 Wahaidi VY, Kowolik MJ, Eckert GJ, Galli DM. Endotoxemia and the host systemic response  
 1202 during experimental gingivitis. *J Clin Periodontol.* 2011;38:412–417. doi: 10.1111/j.1600-  
 1203 051X.2011.01710.x.
- 1204 71 Zhang R, Miller RG, Gascon R, et al. Circulating endotoxin and systemic immune activation in  
 1205 sporadic amyotrophic lateral sclerosis (sALS) *J Neuroimmunol.* 2009;206:121–124. doi:  
 1206 10.1016/j.jneuroim.2008.09.017.
- 1207
- 1208 72 Zhao Y, Jaber V, Lukiw WJ. Secretory products of the human GI tract microbiome and their  
 1209 potential impact on Alzheimer’s disease (AD): detection of lipopolysaccharide (LPS) in AD  
 1210 hippocampus. *Front Cell Infect Microbiol.* 2017;7:318. doi: 10.3389/fcimb.2017.00318.
- 1211 73 Vargas-Caraveo, A., Sayd, A., Maus, S.R. et al. Lipopolysaccharide enters the rat brain by a  
 1212 lipoprotein-mediated transport mechanism in physiological conditions. *Sci Rep* 7, 13113 (2017).  
 1213 <https://doi.org/10.1038/s41598-017-13302-6>
- 1214 74 Jaeger LB, Dohgu S, Sultana R, et al. Lipopolysaccharide alters the blood–brain barrier  
 1215 transport of amyloid  $\beta$  protein: a mechanism for inflammation in the progression of Alzheimer’s  
 1216 disease. *Brain Behav Immun.* 2009;23:507–517. doi: 10.1016/j.bbi.2009.01.017.
- 1217 75 Bryant CE, Spring DR, Gangloff M, et al. The molecular basis of the host response to  
 1218 lipopolysaccharide. *Nat Rev Microbiol.* 2010;8:8–14. doi: 10.1038/nrmicro2266.
- 1219 76 Morris MC, Gilliam EA, Li L. Innate immune programming by endotoxin and its pathological  
 1220 consequences. *Front Immunol.* 2015;5:680. doi: 10.3389/fimmu.2014.00680.

1221 77 Wendeln AC, Degenhardt K, Kaurani L, Gertig M, Ulas T, Jain G, Wagner J, Häsler LM, Wild K,  
1222 Skodras A, Blank T, Staszewski O, Datta M, Centeno TP, Capece V, Islam MR, Kerimoglu C, Staufenbiel  
1223 M, Schultze JL, Beyer M, Prinz M, Jucker M, Fischer A, Neher JJ. Innate immune memory in the brain  
1224 shapes neurological disease hallmarks. *Nature*. 2018;556:332–338. doi: 10.1038/s41586-018-0023-4.

1225 78 Sandiego CM, Gallezot JD, Pittman B, Nabulsi N, Lim K, Lin SF, Matuskey D, Lee JY, O'Connor  
1226 KC, Huang Y, Carson RE, Hannestad J, Cosgrove KP. Imaging robust microglial activation after  
1227 lipopolysaccharide administration in humans with PET. *Proc Natl Acad Sci U S A*. 2015;112:12468–  
1228 12473. doi: 10.1073/pnas.1511003112.

1229 79 Skelly DT, Hennessy E, Dansereau MA, Cunningham C. A systematic analysis of the peripheral  
1230 and CNS effects of systemic LPS, IL-1 $\beta$ , TNF- $\alpha$  and IL-6 challenges in C57BL/6 mice. *PLoS One*.  
1231 2013;8:e69123. doi: 10.1371/journal.pone.0069123.

1232 80. Eigenmann DE, Xue G, Kim KS, Moses AV, Hamburger M, Oufir M. Comparative study of four  
1233 immortalized human brain capillary endothelial cell lines, hCMEC/D3, hBMEC, TY10, and BB19, and  
1234 optimization of culture conditions, for an in vitro blood-brain barrier model for drug permeability  
1235 studies. *Fluids Barriers CNS*. 2013 Nov 22;10(1):33. doi: 10.1186/2045-8118-10-33. PMID: 24262108;  
1236 PMCID: PMC4176484.

1237 81 Belardi B, Hamkins-Indik T, Harris AR, Kim J, Xu K, Fletcher DA. A Weak Link with Actin  
1238 Organizes Tight Junctions to Control Epithelial Permeability. *Dev Cell*. 2020 Sep 28;54(6):792-804.e7.  
1239 doi: 10.1016/j.devcel.2020.07.022. Epub 2020 Aug 24. PMID: 32841596; PMCID: PMC7530003.

1240 82 Tornavaca, O., Chia, M., Dufton, N., Almagro, L. O., Conway, D. E., Randi, A. M., Schwartz, M.  
1241 A., Matter, K., & Balda, M. S. (2015). ZO-1 controls endothelial adherens junctions, cell-cell tension,  
1242 angiogenesis, and barrier formation. *The Journal of cell biology*, 208(6), 821–838.  
1243 <https://doi.org/10.1083/jcb.201404140>

1244 83 Stamatovic, S. M., Johnson, A. M., Keep, R. F., & Andjelkovic, A. V. (2016). Junctional proteins  
1245 of the blood-brain barrier: New insights into function and dysfunction. *Tissue barriers*, 4(1),  
1246 e1154641. <https://doi.org/10.1080/21688370.2016.1154641>

1247

1248